

# REPORT DOCUMENTATION PAGE

Form Approved  
OMB No. 0704-0188

2

Public reporting burden for this collection of information is estimated to average 1 hour per response, including the time for reviewing instructions, searching existing data sources, gathering and maintaining the data needed, and completing and reviewing the collection of information. Send comments regarding this burden estimate or any other aspect of this collection of information, including suggestions for reducing this burden, to Washington Headquarters Services, Directorate for Information Operations and Reports, 1215 Jefferson Davis Highway, Suite 1204, Arlington, VA 22202-4302, and to the Office of Management and Budget, Paperwork Reduction Project (0704-0188), Washington, DC 20503.

1. AGENCY USE ONLY (Leave blank) 2. REPORT DATE 1993 Nov.25 3. REPORT TYPE AND DATES COVERED Final 1 Nov 92 - 31 Oct 93

4. TITLE AND SUBTITLE  
A Fractal Analysis of Near-field Atmospheric Concentration Data  
5. FUNDING NUMBERS  
DAAH04-93-C-0002

6. AUTHOR(S)  
Franklin A. Gifford

7. PERFORMING ORGANIZATION NAME(S) AND ADDRESS(ES)  
F. A. Gifford  
109 Gorgas Lane  
Oak Ridge, TN 37830  
8. PERFORMING ORGANIZATION REPORT NUMBER

SPONSORING/MONITORING AGENCY NAME(S) AND ADDRESS(ES)  
U. S. Army Research Office  
P. O. Box 12211  
Research Triangle Park, NC 27709-2211  
10. SPONSORING/MONITORING AGENCY REPORT NUMBER  
ARO 29192.1-GS-5

11. SUPPLEMENTARY NOTES  
The view, opinions and/or findings contained in this report are those of the author(s) and should not be construed as an official Department of the Army position, policy, or decision, unless so designated by other documentation.

12a. DISTRIBUTION/AVAILABILITY STATEMENT  
Approved for public release; distribution unlimited.  
12b. DISTRIBUTION CODE

3. ABSTRACT (Maximum 200 words)  
A previous study showed that regional and large scale atmospheric motions have Hurst exponents on the order of .4 to .5. The Hurst exponent,  $H$ , equals  $2 - D$ , where  $D$  is the fractal dimension, for a time series. These numbers characterize the degree of irregularity of the time-series. Hurst exponents were calculated for a large number of concentration-time series from several sources, whose sampling times ranged from 6 seconds to 1 hour. Hurst exponents for these data ranged from about .2 to .4. Such values indicate that the small-scale, near-field turbulent eddies differ qualitatively from the larger-scale motions, for which  $H$  approaches the value .5, the value for Brownian motion. Since models in effect assume the value  $H = .5$  in turbulence parameterizations, these results suggest that smaller, realistic  $H$ -values, appropriate to planetary boundary layer turbulence, should be used to parameterize turbulence.

94 2 07 124

14. SUBJECT TERMS  
Atmospheric turbulence; planetary boundary diffusion; fractal dimension; Hurst exponent; diffusion models.  
15. NUMBER OF PAGES  
layer; plume  
16. PRICE CODE

17. SECURITY CLASSIFICATION OF REPORT UNCLASSIFIED  
18. SECURITY CLASSIFICATION OF THIS PAGE UNCLASSIFIED  
19. SECURITY CLASSIFICATION OF ABSTRACT UNCLASSIFIED  
20. LIMITATION OF ABSTRACT UL

94-04270

AD-A275 460

DTIC QUALITY INSPECTED 1

DTIC ELECTE FEB 09 1994

**Best  
Available  
Copy**

CONTENTS

|  | <u>PAGE NO.</u> |
|--|-----------------|
| 1. INTRODUCTION.....                             | 4               |
| 2. FRACTAL DIMENSION AND THE HURST EXPONENT..... | 5               |
| 3. SMALL-SCALE DIFFUSION DATA.....               | 6               |
| 4. RENORMALIZED-RANGE ANALYSIS.....              | 8               |
| 5. HOURLY-AVERAGED CONCENTRATION DATA.....       | 10              |
| 6. SHORT-PERIOD AVERAGED CONCENTRATION DATA..... | 11              |
| 7. DISCUSSION.....                               | 13              |
| 8. CONCLUSIONS.....                              | 13              |
| 9. ACKNOWLEDGMENTS.....                          | 14              |
| 10. BIBLIOGRAPHY.....                            | 15              |

FIGURE LEGENDS

Figures 1 to 4: Typical concentration-time series for the four atmospheric data sets; TVA87, CSIRO85, CSIRO89, and Washington State U., cf Table I for details.

Figure 5: Twelve-hour averaged  $Kr^{H=}$  concentrations at Murray Hill, NJ (MUR). Concentration units are picocuries/m<sup>3</sup>. Time is given in half-hour periods. (From Gifford, 1991).

Figure 6: Wind-tunnel concentration-time series based on half-second sampling, by NOAA/ARL, Atmospheric Sciences Modeling Div., Research Triangle Park, NC. Run #35

Figures 7 to 14: Renormalized-range analyses of hourly-averaged SO<sub>2</sub> concentration data from stations around the TVA Cumberland Steam Plant (see Table III).

Figure 15: Renormalized-range analysis of twelve-hour averaged  $Kr^{H=}$  concentrations measured at Tarboro, NC (TAR), from Gifford (1991).

Figures 16 to 33: Renormalized-range (R/S) analyses of short-period averaged concentration data from the various sources described in Tables I and IV. The dashed lines represent best power-law fits of each R/S curve to Eq.3; values of the Hurst exponent, H, so defined are given in Table IV.

TABLES

TABLE I: SOURCES OF SHORT-TERM AVERAGED CONCENTRATION-TIME SERIES.....7

TABLE II: VALUES OF THE HURST EXPONENT, H, SPECTRAL SLOPE,  $\beta$ , AND FRACTAL DIMENSION, D, FOR TIME SERIES.....9

TABLE III: CUMBERLAND STEAM PLANT SO<sub>2</sub> MONITORING STATIONS...10

TABLE IV: SUMMARY OF FRACTAL VALUES FROM CONCENTRATION-TIME SERIES USING EQ. (3).....12

|                                     |                      |
|-------------------------------------|----------------------|
| <input checked="" type="checkbox"/> |                      |
| Unannounced Justification .....     |                      |
| By .....                            |                      |
| Distribution / .....                |                      |
| Availability Codes                  |                      |
| Dist                                | Avail and/or Special |
| A-1                                 |                      |

1. INTRODUCTION

The scales and structure of turbulent atmospheric motions differ considerably from those of theoretically idealized turbulent flows, such as stationary, homogeneous turbulence, or unbounded shear flows, and from their laboratory simulations. Atmospheric turbulent motions consist of large, essentially two-dimensional, random eddy motions with scales of several hundred kilometers or more superimposed on a field of smaller eddies that become more three-dimensional the smaller their scale. The former cascade eddy enstrophy (mean-squared vorticity) from the very large (several thousands of kilometers) scale of eddy-energy generation to scales of a few hundred kilometers, and the latter cascade eddy energy to the dissipative scale (< 1 cm). The effects of these quite different kinds of eddy motions can be seen in the atmospheric diffusion of natural and anthropogenic effluent clouds released into the atmosphere. Small-scale, three-dimensional eddies rapidly spread and dilute effluent clouds; large-scale, two-dimensional eddies rapidly distort them (Gifford 1985, 1989).

It was proposed (Gifford 1982, 1984) that the boundary between these two scales of atmospheric turbulent motions is measured by the Lagrangian integral time-scale of the turbulence, and it was shown that this scale is essentially equal to the reciprocal of the Coriolis parameter, equal to about 3 hours in mid-latitudes. Eddies having larger time-scales distort diffusing clouds; eddies having smaller time-scales are responsible for the diffusive cloud spreading. The boundary is of course broad, not sharp. The essential correctness of this proposition is attested to by a variety of observations of large atmospheric clouds and plumes (Barr and Gifford 1987, Gifford, 1983).

A previous study was undertaken (Gifford 1991) in an attempt to apply a method of fractal geometry to a long series of 12-hourly averaged  $K_{r=}$  concentrations measured at 5 points extending downwind from the Savannah River plant at Aiken, SC, the most distant being Murray Hill, NJ, about 1100km from the source. By calculating the so-called Hurst exponent,  $H$ , for these data time-series, it was possible to estimate the fractal dimension of atmospheric motions at these large scales. The previous report provides a brief survey of the basic fractal-geometry concepts involved in this analysis as well as pertinent literature citations. The present study attempts to extend the large-scale results to smaller-scale, atmospheric boundary-layer turbulence by analyzing a variety of sets of smaller-scale atmospheric diffusion data.

## 2. FRACTAL DIMENSION AND THE HURST EXPONENT

An object's fractal dimension has been called a measure of its irregularity (Ludwig, 1989). The Euclidean dimension of a circle or other plane figure is, for example, two; but many planar objects, especially in nature, are not very well characterized by their Euclidean dimension, for instance the radar plot of a precipitation band. Mandelbrot (1982) devised fractal geometry to deal with this kind of problem, and it has proved to be a very useful concept. The central property of a fractal object is that,

if it is viewed over a range of resolutions (scales), its shape is observed to possess the property of self-similarity. The degree of its irregularity is measured by the fractal dimension involved. The fractal dimension of the perimeter of a radar image of a cloud or rain band has, for example, been found to equal 1.35 (and of its area, 2.35) to linear scales up to several hundred kilometers (Lovejoy, 1982).

Long time series of pollutant concentrations measured downwind from a source contain information on the structure of turbulence in the two- and three-dimensional cascade ranges of atmospheric turbulence and so can be expected to be related to the fractal dimension of atmospheric flows in these ranges. For a concentration-time series  $C(t)$  to be self-similar, changes in concentration at a given point must depend on time in such a way that, statistically speaking, for any two times  $t_1$  and  $t_2$ ,

$$C(t_2) - C(t_1) \propto (t_2 - t_1)^H \quad (1)$$

where  $H$  is the similarity constant, called the Hurst exponent.  $H$  is related to the fractal dimension,  $D$ , by

$$D = 2 - H \quad (2)$$

Results from the previous study (Gifford 1991) of the ACURATE data showed that the Hurst exponent for regional-scale atmospheric turbulence lies in the range  $H=0.35$  to  $0.45$ , and there was some indication of slightly higher values, to  $H=.48$ , at the largest scales (about 1000 km) measured by these data. The remainder of the present report describes the results of a study of Hurst exponents derived from smaller-scale atmospheric concentration measurements.

### 3. SMALL-SCALE DIFFUSION DATA

Atmospheric concentration measurements were obtained from the following sources: 1) Hourly SO<sub>2</sub> concentration measurements made at monitoring stations in the vicinity of the TVA's Cumberland, TN. Steam Plant for the year 1987 (Gautney, 1989); 2) Ten-second averages of NO concentrations measured over 3- to 4-hour periods in the vicinity of two elevated sources in Australia by the CSIRO Div. of Coal and Energy Technology in 1989 (Carras, 1993); 3) Six-second averages of SF<sub>6</sub> concentrations obtained at distances of from 25 to 100 m downwind from a source at a CSIRO field site in Australia, described by Sawford (1987) and previously analyzed by him and by Hanna and Insley (1989); 4) Six series of 0.1-second averages of SF<sub>6</sub> concentrations measured over 10-minute periods at various distances up to 700 m downwind from a ground-level source at a flat, desert site in southwestern Washington (Peterson, 1989). 5) Two runs from a group of wind-tunnel plume measurements of ethane concentrations at two distances from the source, made at 1/2-second intervals for 300 second periods (Lawson 1993). Relevant information about all these concentration data sources is summarized in TABLE I.

TABLE I  
SOURCES OF SHORT-TERM AVERAGED  
CONCENTRATION-TIME SERIES

|           | <u>TVA87</u> | <u>CSIRO89</u> | <u>CSIRO85</u> | <u>Wash.State U.</u> | <u>NOAA/ARL WIND<br/>TUNNEL DATA</u> |
|-----------|--------------|----------------|----------------|----------------------|--------------------------------------|
| Source    |              |                |                |                      |                                      |
| Type      | Stack        | Stack          | Surface        | Surface              | Elevated                             |
| Receptor  |              |                |                |                      |                                      |
| Distance: | 2-11km       | 5-10km         | 25-100m        | 160-700m             | ≈ 1-3 m                              |
| Duration  |              |                |                |                      |                                      |
| of Runs : | 1 yr         | 3-4 hr         | 1 hr           | 10 min               | 300 s                                |
| Averag-   |              |                |                |                      |                                      |
| ing time: | 1 hr         | 10 sec         | 6 sec          | 0.1 sec              | .5 s                                 |
| No. Runs  |              |                |                |                      |                                      |
| Analyzed: | 17           | 4              | 7              | 4                    | 2                                    |

About half the total available atmospheric data were

analyzed in this study. Runs were omitted if they contained significant periods of missing data, or if they were too short. Runs were selected for analysis to bring out possible trends in the results, such as seasonal variability (TVA data), or boundary-layer stability effects (Washington State U. data). Figures 1-4 illustrate typical concentration-time series from these four atmospheric data sets and bring out some interesting points. Fig. 1 is based on hourly averages of  $\text{SO}_2$  concentrations during the period January through March from Station 7, about 8 km SSW of TVA's Cumberland Steam Plant. It shows the same noisy background, punctuated by brief concentration spikes, as for instance the Murray Hill data, Fig. 5 from the previous study (Gifford 1991) of the 12-hour averaged ACURATE data. Figs. 3 and 4, whose data averaging times are very short, have overall much more consistently noisy concentration-time traces and, interestingly, more resemble the NOAA/ARL wind-tunnel data, an example of which is shown in Fig. 6. The object of the present study is to see what further, quantitative structural information can be gleaned from these noisy, seemingly random concentration-time series.

#### 4. RENORMALIZED RANGE ANALYSIS

The "renormalized-range" statistic (Mandelbrot 1982) is given, from Eq. 1, by

$$R(\tau)/S(\tau) = [(C_{\max}(\tau) - C_{\min}(\tau)]/\sigma_c(\tau) = b\tau^H, \quad (3)$$

where  $R$  is the range of  $C$ , and  $S$  ( $=\sigma_c$ ) is its standard deviation, during the time period  $\tau = t_1 - t_0$ ,  $b$  is a constant, and the time interval  $\tau$  is measured from the beginning of the series. If atmospheric turbulent motions are self-similar, a logarithmic plot of  $R/S$  and  $\tau$  should from Eq. 3 contain broad linear ranges with slopes equal to  $H$ , the Hurst exponent. Moreover in general  $D = E+1-H$  (Mandelbrot 1982) and so the fractal dimension,  $D$ , is also determined by this procedure.

The concept of similarity regions of the atmospheric energy

spectrum is quite familiar, so it is not surprising to find that the similarity exponent  $H$  is also related to the slope  $1/f^\beta$  of the spectrum in the similarity range,  $f$  being frequency. It follows that for time series

$$D = E + 1 - H = E + (3-\beta)/2 \quad (4)$$

according to Mandelbrot (1982). From this the values of  $H$ ,  $D$ , and  $\beta$  for time series of concentrations (for which  $E = 1$ ) can be summarized as in TABLE II, from Gifford (1991).

TABLE II

THEORETICAL VALUES OF THE HURST EXPONENT,  $H$ , SPECTRAL SLOPE,  $\beta$ , AND FRACTAL DIMENSION,  $D$ , FOR TIME SERIES

| Power Law:<br>Parameter: | Extreme:<br>Value | Kolmogoroff:<br>Turbulence | Brownian:<br>Motion | Extreme<br>Value. |
|--------------------------|-------------------|----------------------------|---------------------|-------------------|
| H                        | 0                 | 1/3                        | 1/2                 | 1                 |
| $\beta$                  | 1                 | 5/3                        | 2                   | 3                 |
| D                        | 2                 | 5/3                        | 3/2                 | 1                 |

Table II shows how the renormalized-range analysis of concentration time-series can provide useful information on atmospheric turbulence structure that is directly related to more familiar structural concepts, such as the shape of the energy spectrum of the flow.

Lagrangian trajectory models commonly assume that the stochastic element in air-parcel motions is described by ordinary Brownian motion, which corresponds to a Hurst exponent of  $H = 1/2$ . Similarly, Eulerian grid models use what amounts to the same assumption to characterize sub-grid scale motions. The R/S analysis can provide a check on this assumption. Moreover methods have been devised (see e.g. Feder, 1988, Turcotte, 1989 for instance) by means of which actual values of  $H$  might be introduced into atmospheric models.

## 5. HOURLY-AVERAGED CONCENTRATION DATA

The SO<sub>2</sub> monitoring stations around the TVA Cumberland Steam Plant are located as shown in TABLE III. Figures 7 through 14

TABLE III  
CUMBERLAND (TVA) STEAM PLANT SO<sub>2</sub> MONITORING STATIONS

| <u>Station Number</u> | <u>Source Distance</u> | <u>Direction</u> |
|-----------------------|------------------------|------------------|
| 7                     | 8.1 km                 | SSW              |
| 10                    | 7.4 km                 | SE               |
| 18                    | 10.6 km                | NE               |
| 23                    | 2.7 km                 | SW               |
| 24                    | 6.4 km                 | WSW              |

illustrate the results of renormalized-range, R/S analysis of Cumberland data based on Eq. 3. Figs. 7 through 10 are based on January through March data, and Figs. 11 through 14 are for April through June data. These R/S curves are based on data series of 600 to 1000 values. Gaps in the records prevented use of other data periods for R/S analysis.

The Cumberland hourly data are seen to yield R/S-curves that are qualitatively similar to those based on the 12-hour averaged Kr<sup>ms</sup> concentration data analyzed earlier (Gifford 1991). Figure 15 from that report, the R/S analysis of the Tarboro, NC, data, is representative of the ACURATE results. Periods of steady rise of the R/S-values, with slope-values indicating H-exponents around 0.40, are punctuated by sharp breaks, presumably caused by "pluming" (direct passage of the plume over the station), or other major shifts in the driving meteorological conditions. The main qualitative difference is the time-scale of the events. There is some indication that the 12-hour averaged ACURATE data have slightly higher H-values (.4-.5) than the 1-hour averaged TVA data (.35 to .4).

## 6. SHORT-PERIOD AVERAGED CONCENTRATION DATA

Figures 16 through 33 contain the R/S-analyses that have been performed on short-term time-averaged atmospheric concentration data from the two CSIRO sets and the Washington State U. data, and two examples from the NOAA/ARL wind-tunnel plume data. Slopes, that is values of Hurst exponents  $H$ , indicated by the dashed lines of best fit in all these Figures are summarized in Table IV.

TABLE IV  
SUMMARY OF FRACTAL VALUES FROM CONCENTRATION-  
TIME SERIES USING (EQ.3)

| Station                                   | Series Length | b            | H    | D     |
|---|---------------|--------------|------|-------|
| (JFM 1987 TVA Cumberland Steam Plant)     |               |              |      |       |
| 07  | 827           | 1.45         | .34  | 1.66  |
| 10  | 606           | 0.81         | .45  | 1.55  |
| 18  | 1646          | 1.12         | .33  | 1.67  |
| 24  | 852           | 1.08         | .40  | 1.60  |
|   |               | (Avg. = 1.12 | .38  | 1.62) |
| (AMJ 1987 TVA Cumberland Steam Plant)     |               |              |      |       |
| 10  | 637           | 1.04         | .44  | 1.56  |
| 18  | 701           | 2.07         | .25  | 1.75  |
| 23  | 702           | 1.00         | .40  | 1.60  |
| 24  | 702           | 0.74         | .45  | 1.55  |
|   |               | (Avg. = 1.21 | .38  | 1.62) |
| (CSIRO 1985)                              |               |              |      |       |
| 1   | 580           | 2.44         | .12  | 1.88  |
| 3   | 590           | 1.97         | .17  | 1.83  |
| 14  | 595           | 2.97         | .06  | 1.94  |
| 19  | 646           | 2.76         | .10  | 1.90  |
| 26  | 597           | 2.24         | .12  | 1.88  |
| 39  | 562           | 1.90         | .15  | 1.85  |
| 41  | 235           | 1.57         | .26  | 1.74  |
|   |               | (Avg. = 2.76 | .14  | 1.86) |
| (CSIRO 1989)                              |               |              |      |       |
| B   | 1310          | 1.90         | .14  | 1.86  |
| C   | 1316          | 1.14         | .26  | 1.74  |
| D   | 1120          | 2.12         | .14  | 1.86  |
| E   | 1157          | 1.32         | .22  | 1.78  |
|   |               | (Avg. = 1.62 | .19  | 1.81) |
| (Washington State U., Desert Study, 1987) |               |              |      |       |
| 4   | 2999          | 1.88         | .14  | 1.86  |
| 25  | 3000          | 2.03         | .11  | 1.89  |
| 27  | 2996          | 4.18         | -.03 | --    |
| 34  | 2999          | 3.16         | .05  | 1.95  |
| 40  | 1836          | 1.97         | .12  | 1.88  |
|   |               | (Avg. = 2.64 | .08  | 1.92) |
| (NOAA/EPA Wind Tunnel Plume Study, 1991)  |               |              |      |       |
| 35  | 3498          | 1.16         | .28  | 1.72  |
| 36  | 569           | 1.23         | .24  | 1.76  |

Table IV, and the Figures it accompanies, are the principal results of this renormalized-range analysis.

## 7. DISCUSSION

Taken together with the previous (Gifford 1991) H-values based on 12-hour average concentration data, Table IV shows that concentration-time series characteristic of typical small-scale, surface boundary-layer turbulence are measured by Hurst exponents in the range .1 to .2. For the larger scale of boundary-layer turbulence events measured by the hourly-averaged TVA data, H values of about .35 to .4 are calculated by the R/S technique. Such values are, according to Table II, typical of locally homogeneous turbulence (Kolmogoroff turbulence). Hentschel and Procaccia (1983) present an interesting theoretical discussion of this kind of turbulence based on considerations of fractal geometry and conclude that H is close to .35 for this type. At turbulence scales large enough to affect the 12-hour averaged concentration values of the ACURATE data, yet larger H-values are found, in the range .4 to .45, particularly at scales of from several days to weeks. Random turbulence at these larger scales is two dimensional; it deforms, rather than diffuses pollutant clouds.

No seasonal difference was detected in the Cumberland R/S analyses for the two quarterly data periods that could be examined (late winter and early spring). As to variation with stability conditions, the short-range data from Washington State U. covered a range of conventional boundary layer stability categories as follows: run 4, quite unstable, type A; runs 25 and 27, stable, type E; run 34, very stable, type G; run 40, near neutral, type D. The Table IV results suggest that the stable runs are associated with somewhat smaller H-exponents than unstable and neutral runs.

## 8. CONCLUSIONS

There seems little doubt, based on the above renormalized-range analysis of a large amount of concentration time-series data gathered over a wide range of plume-diffusion scales, that the characteristic fractal dimension of diffusing plumes from sources in the boundary layer increases with diffusion time ("plume-age",

or downwind evolution of the diffusing cloud). The characteristic Hurst-exponent  $H$  equals about  $.3 \pm .1$  in the boundary layer. This controls the near-field of diffusion, to distances on the order of a few tens of kilometers downwind, the range of rapid cloud spreading in the 3-D, energy-cascade region of atmospheric turbulence. As a diffusing cloud spreads to larger scales, to distances of several hundreds of kilometers, it continues to be diffused by these smaller-scale eddies but becomes more and more rapidly deformed by the larger, 2-D, enstrophy-cascading eddies. The characteristic Hurst-exponent of these large-scale, 2-D turbulent atmospheric motions seems to be in the range  $H=.4-.5$ , approaching that of Brownian motion (white noise). The difference between such white-noise turbulence and the "red-noise" turbulence characterized by  $H=.2$  or  $.3$ , which according to Table IV is characteristic of near-field boundary-layer diffusion, can be considerable (Gifford 1991, Fig. 7). Adjustment of stochastic elements in atmospheric turbulence and diffusion models to account for this difference from the standard modeling assumption, in effect that  $H = 1/2$ , should be considered seriously.

## 9. ACKNOWLEDGMENTS

The writer would like to express his sincere thanks to the following persons who, promptly and unselfishly, supplied the concentration data, in several cases previously unreported, on which this report is based: Drs. John Carras, Div. of Coal and Energy Technology, CSIRO, Australia; Larry L. Gautney, Jr., TVA; Steven R. Hanna, Sigma Research Corp.; Robert E. Lawson, Jr., Atmospheric Sciences Modeling Div., NOAA/ARL; and Holly G. Peterson, Laboratory for Atmospheric Research, Washington State University.

The writer, F. A. Gifford, an independent, self-employed research worker, is the only participant in this project. The research involved no subcontracts, and no inventions or advanced degrees have resulted.

## 10. BIBLIOGRAPHY

- Barr, S. and F. A. Gifford, 1987: The random force theory applied to regional scale atmospheric diffusion, Atmos. Environ., 21, 1737-1741.
- Carras, J., 1993: Personal Communication.
- Feder, J., 1988: Fractals, 283pp, Plenum Press, NY.
- Gautney, L. L., Jr., 1989: Personal Communication.
- Gifford, F. A., 1982: Horizontal diffusion in the atmosphere: a Lagrangian, dynamical theory, Atmos. Environ., 16, 505-512.
- Gifford, F. A., 1983: Atmospheric diffusion in the mesoscale range: the evidence of recent plume width observations, Preprint Vol., 6th Symp. on Turbulence and Diffusion, March 22-25, 1983, Amer. Meteor. Soc.
- Gifford, F. A., 1984 The random-force theory: application to meso- and large-scale atmospheric diffusion, Boundary Layer Meteor., 30, 159-175.
- Gifford, F. A., 1985: Atmospheric diffusion in the range 20 to 2000 km, in Air Poll. Modeling and its Applications, Plenum Press, 247-265.
- Gifford, F. A., 1989: The shape of large tropospheric clouds, or "Very like a whale", Bull. Am. Meteor. Soc., 70, 468-475.
- Gifford, F. A., 1991: The structure of atmospheric diffusion at regional scales. Final Tech. Rep., U. S. Army Res. Office, Contract No. P-27096-GS-S, 37pp.
- Hanna, S. R. and E. M. Insley, 1989: Time series analysis of concentration and wind fluctuations. Boundary-Layer Meteorology, 47, 131-147.
- Hentschel, H. G. E. and I. Procaccia, 1983: Fractal nature of turbulence as manifested in turbulent diffusion. Phys. Rev. Letters, A, 27, 1266-1269.
- Ludwig, F., 1989: Atmospheric fractals, a review, Environ. Software, 4, No. 1 (March, 1989).
- Lawson, R. E., Jr., 1993: Personal Communication.
- Mandelbrot, B. B., 1982: The Fractal Geometry of Nature, 486 pp, W. H. Freeman Co., NY.
- Peterson, H. G., 1989: Personal Communication.
- Sawford, B. L., 1987: Conditional Concentration Statistics for

Surface Plumes in the Atmospheric Boundary Layer. Boundary-Layer Meteorol., 38, 209-223.

Turcotte, D. L., 1989: Fractals in geology and geophysics, in Fractals in Geophysics, 171-196, Birkhauser Verlag, Basel.

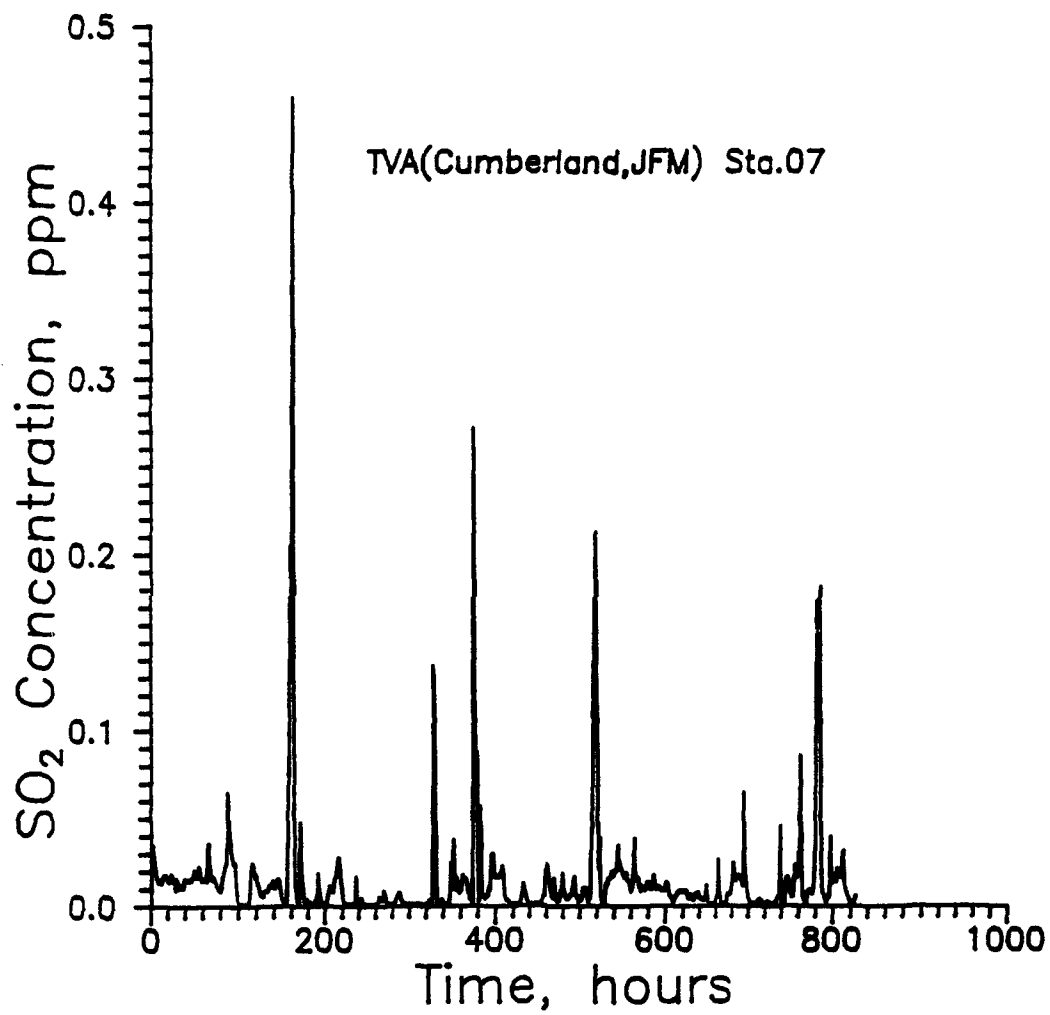


Figure 1

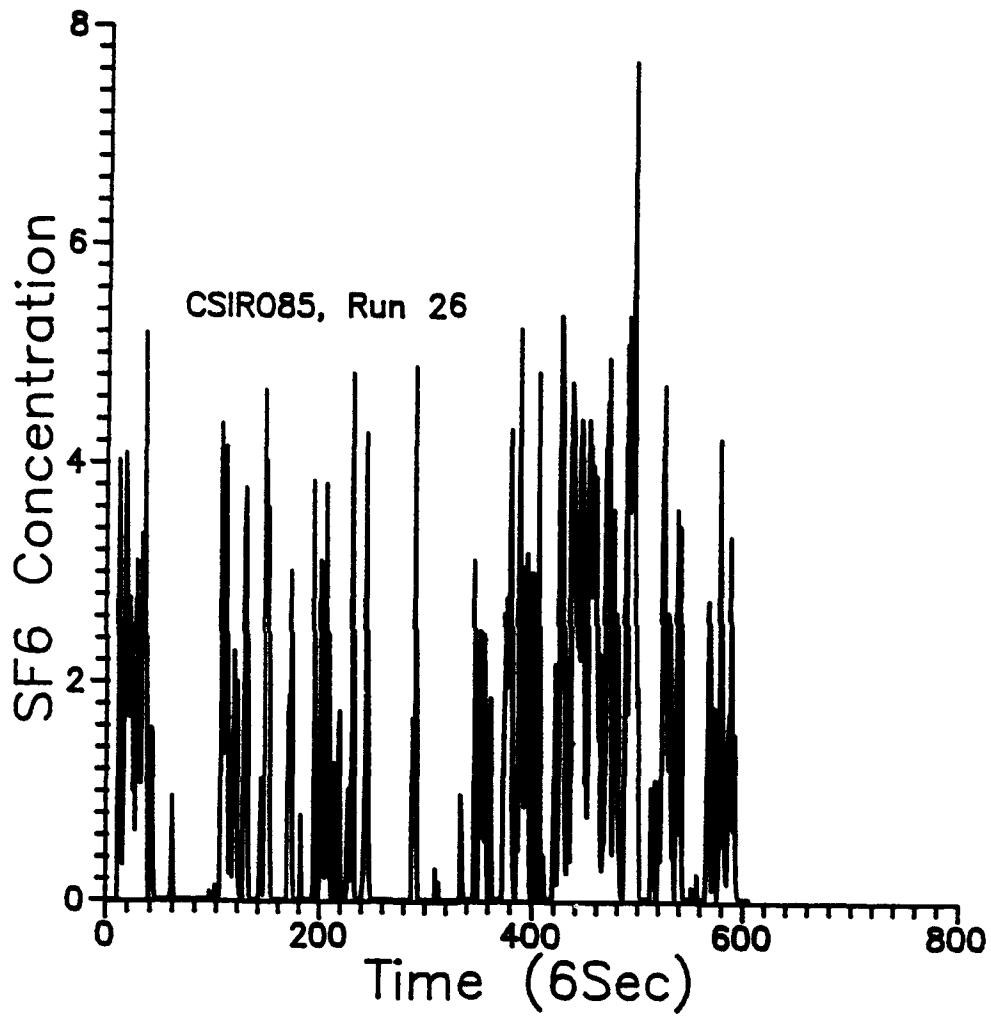


Figure 2

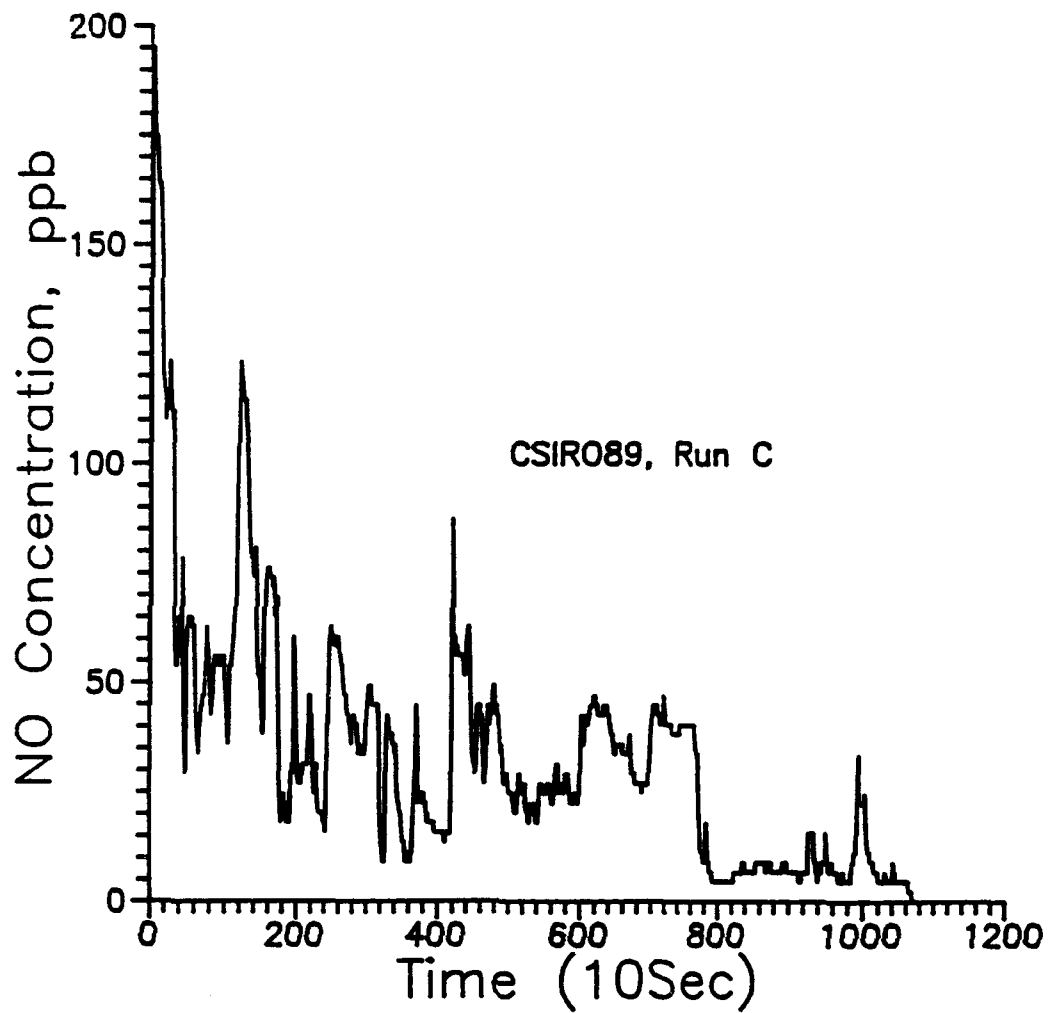


Figure 3

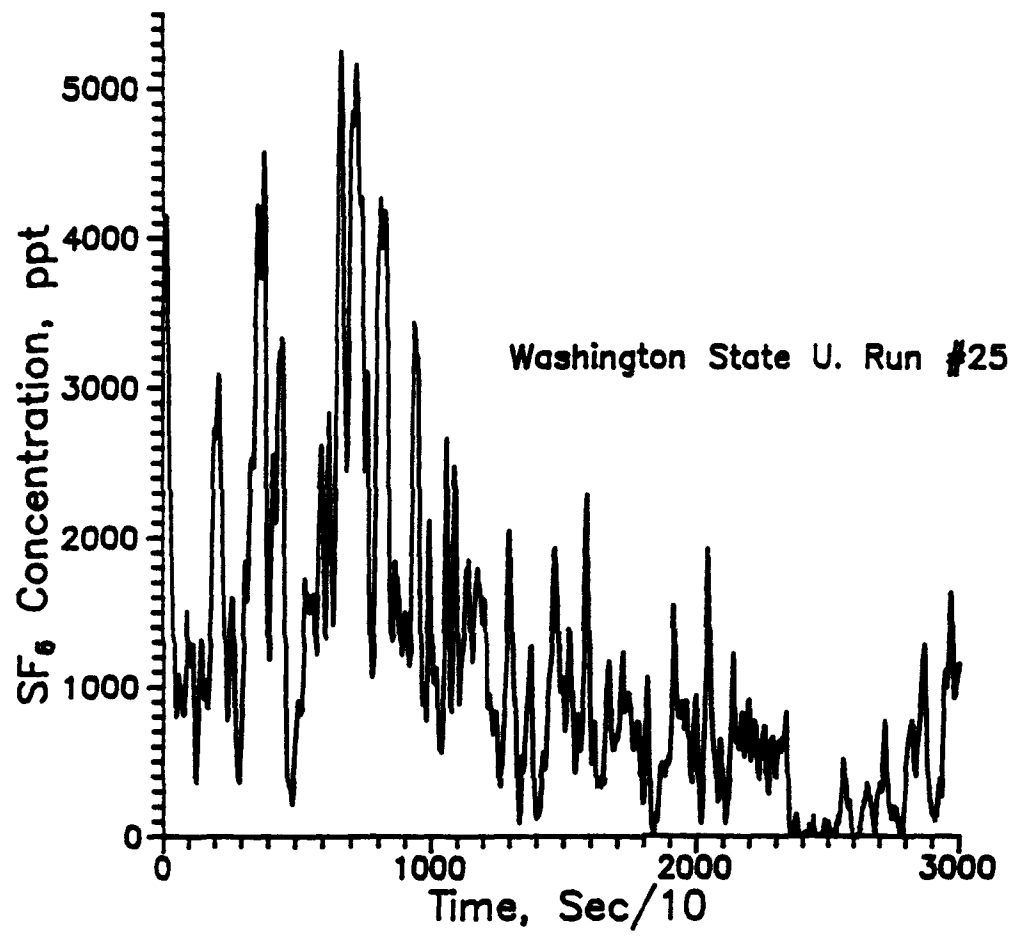


Figure 4

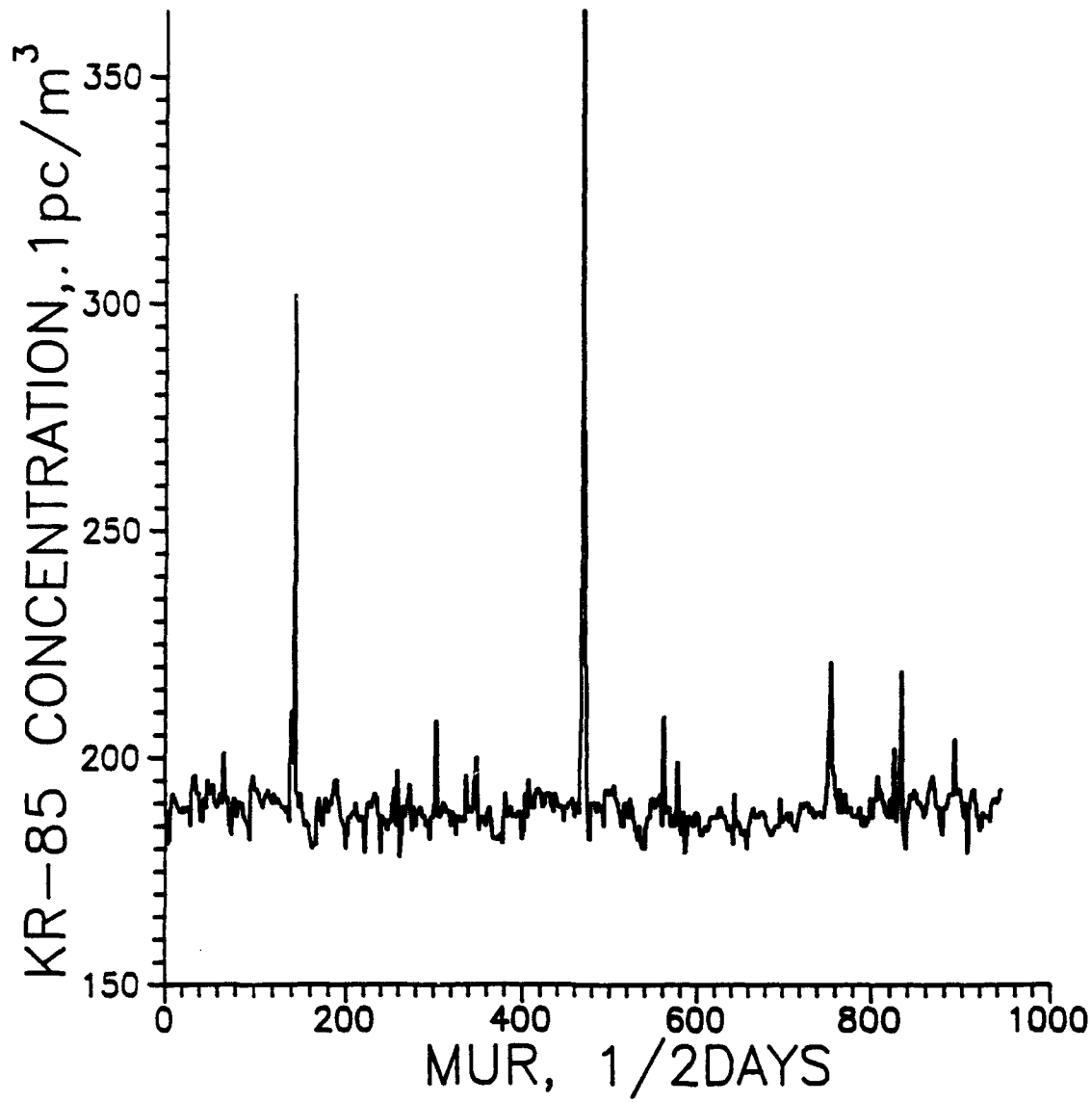


Figure 5

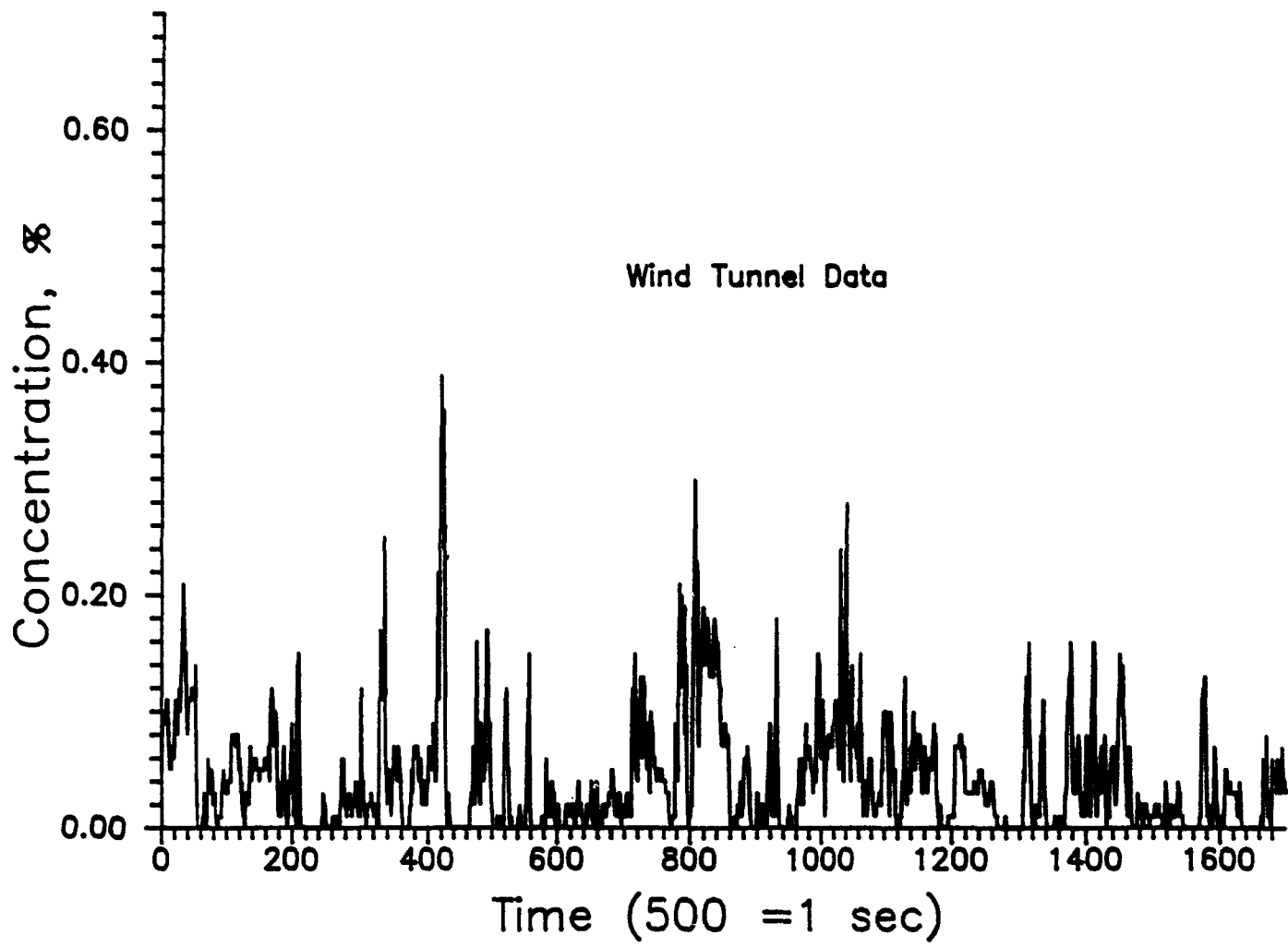


Figure 6

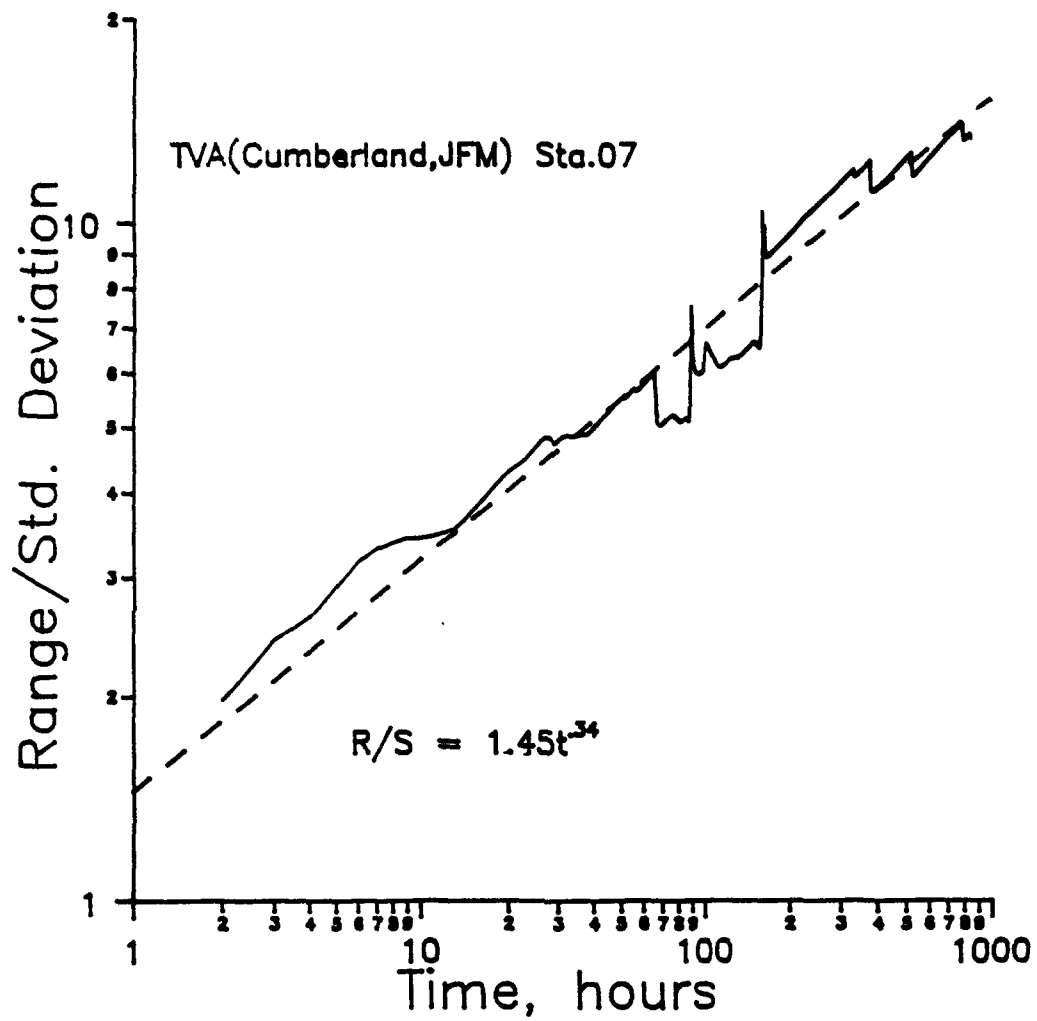


Figure 7

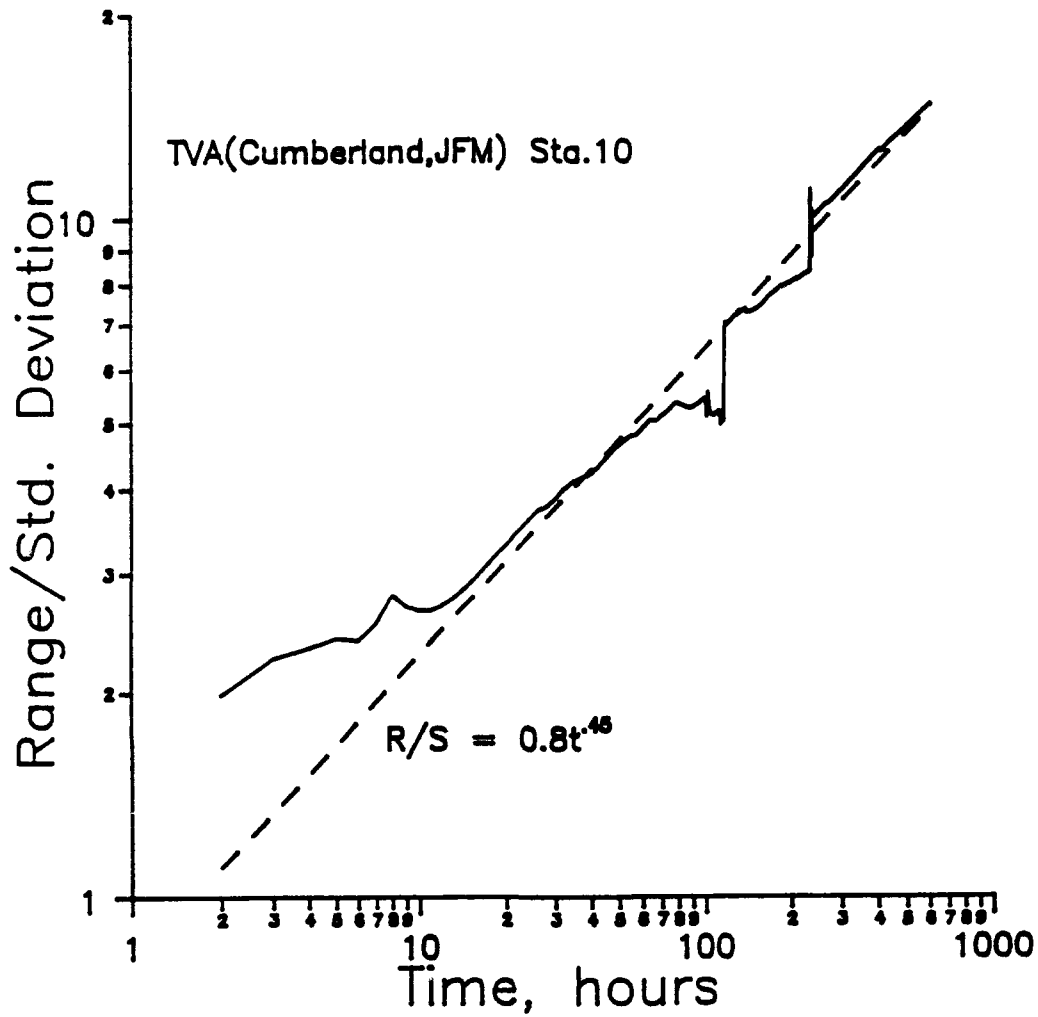


Figure 8

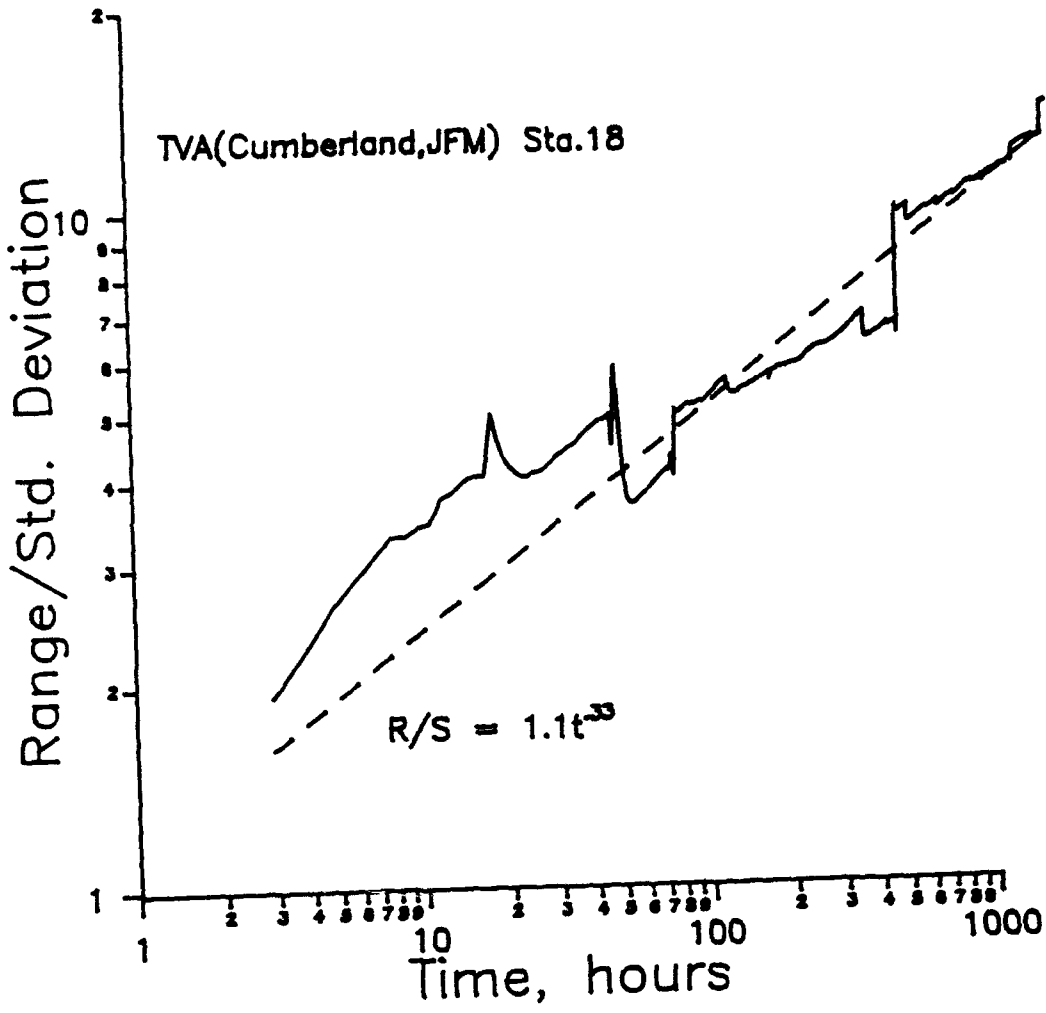


Figure 9

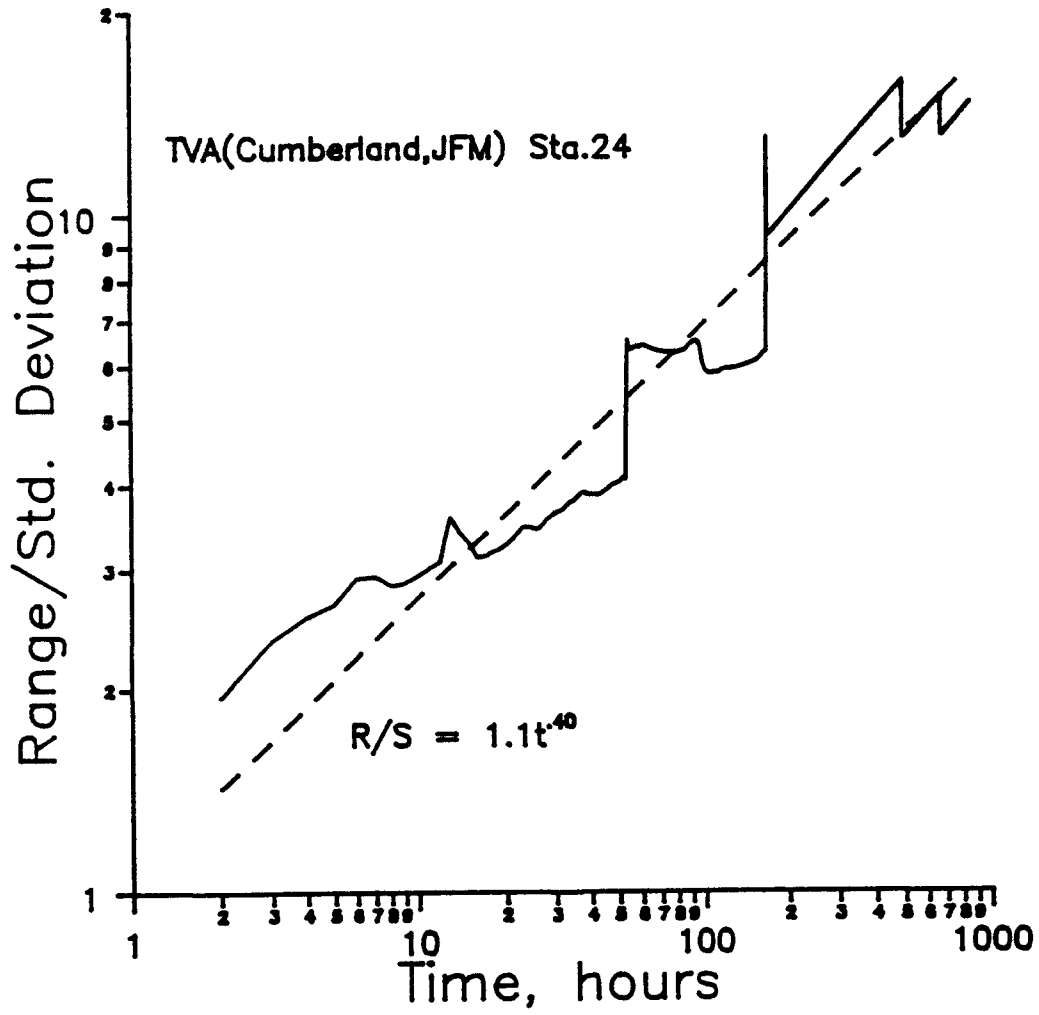


Figure 10

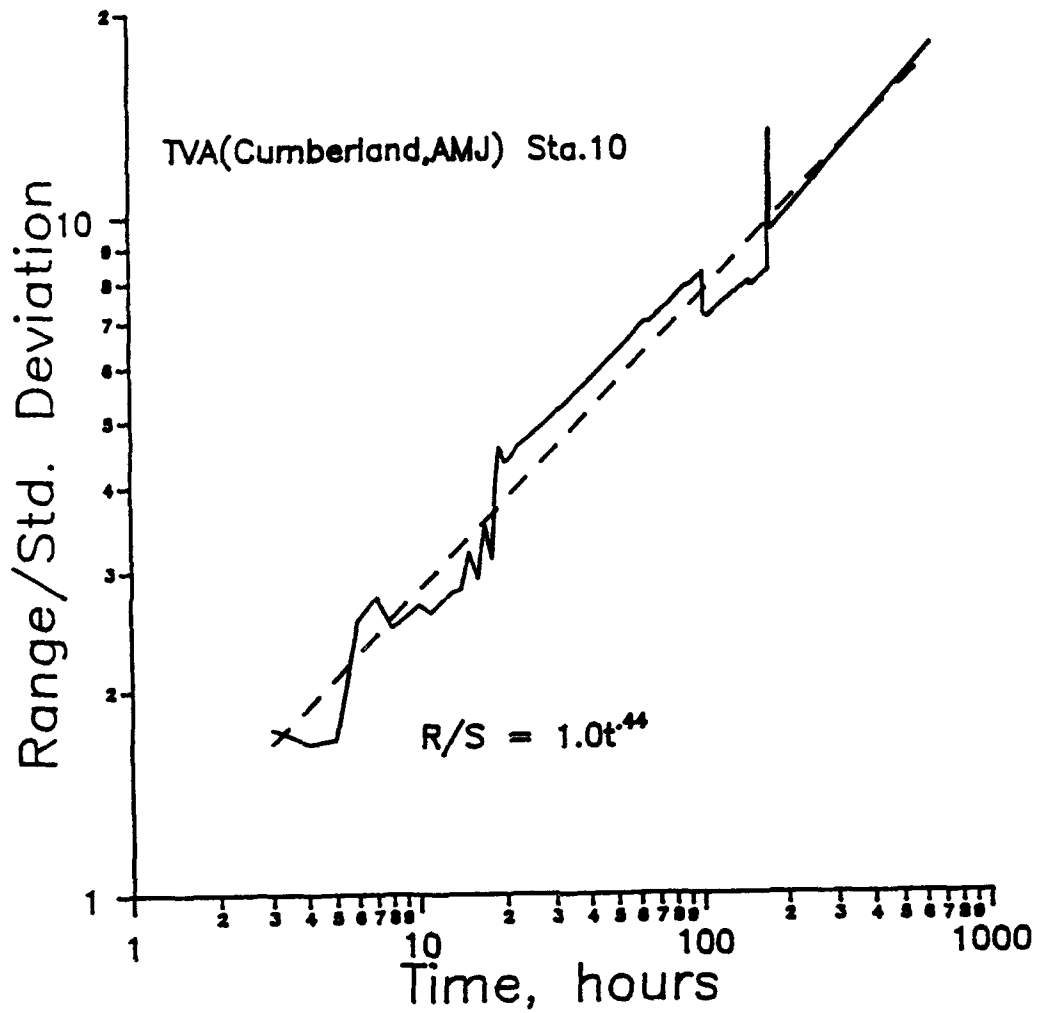


Figure 11

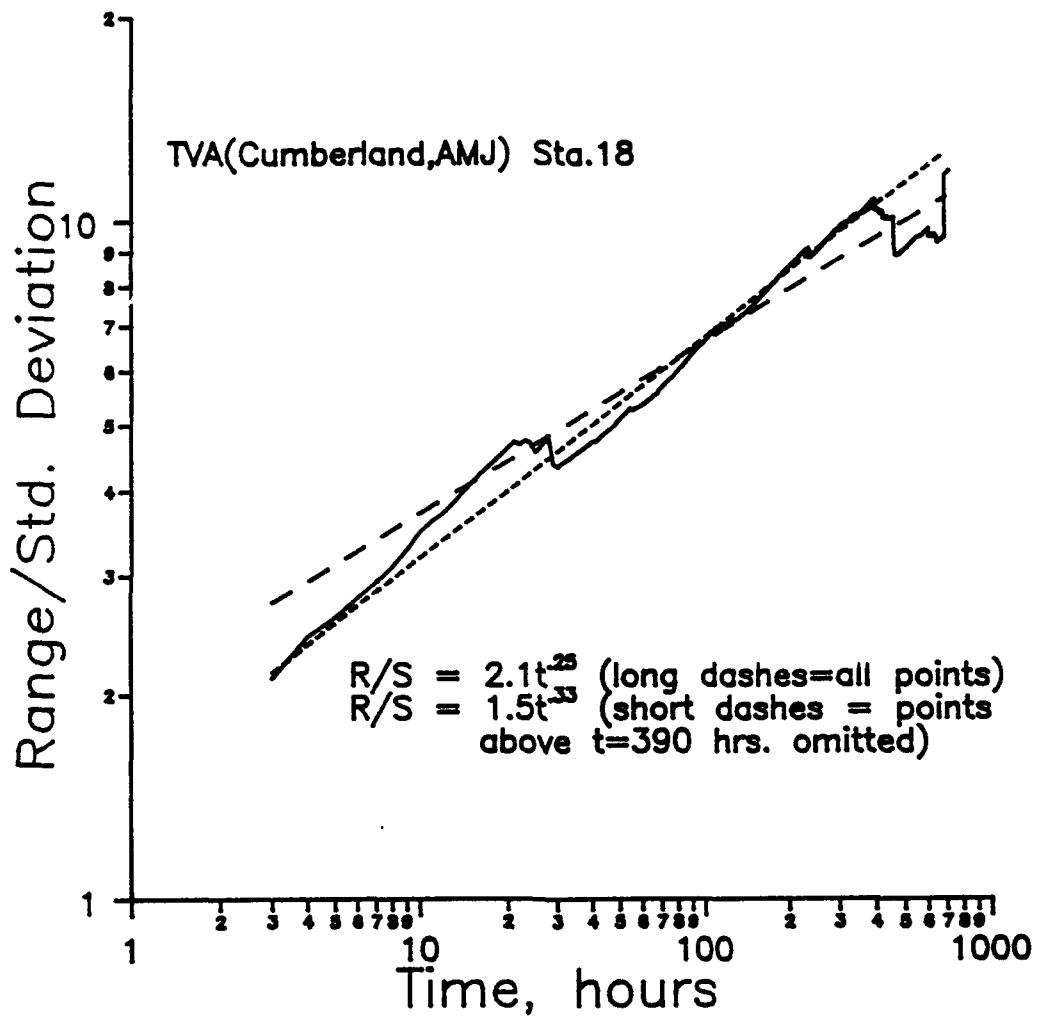


Figure 12

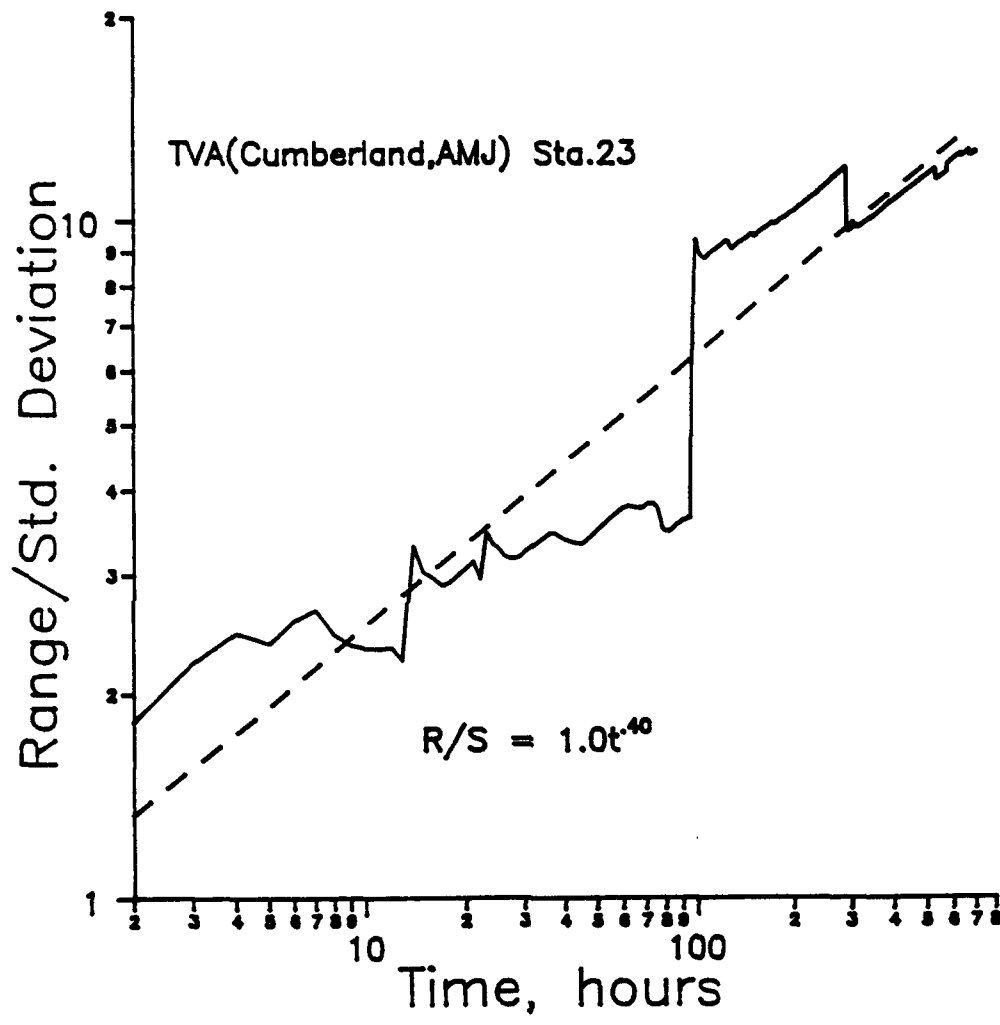


Figure 13

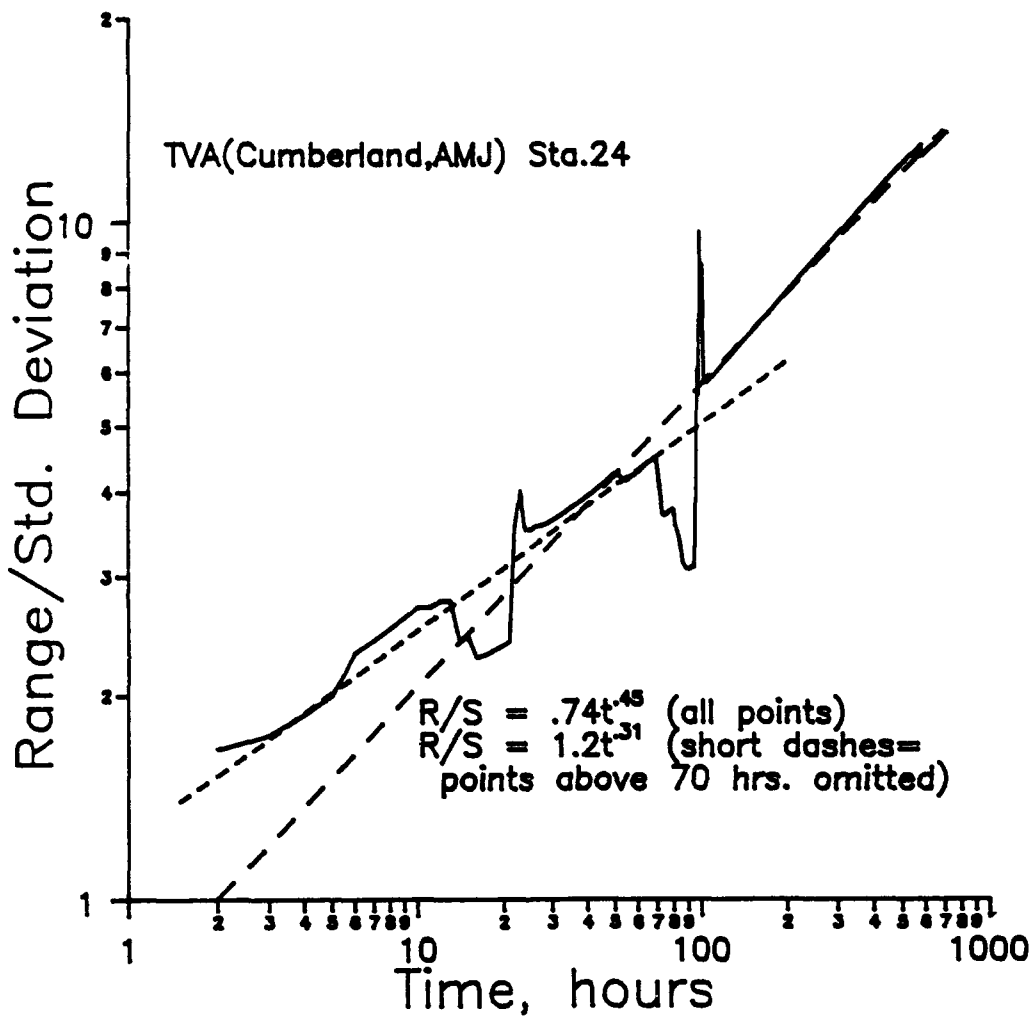


Figure 14

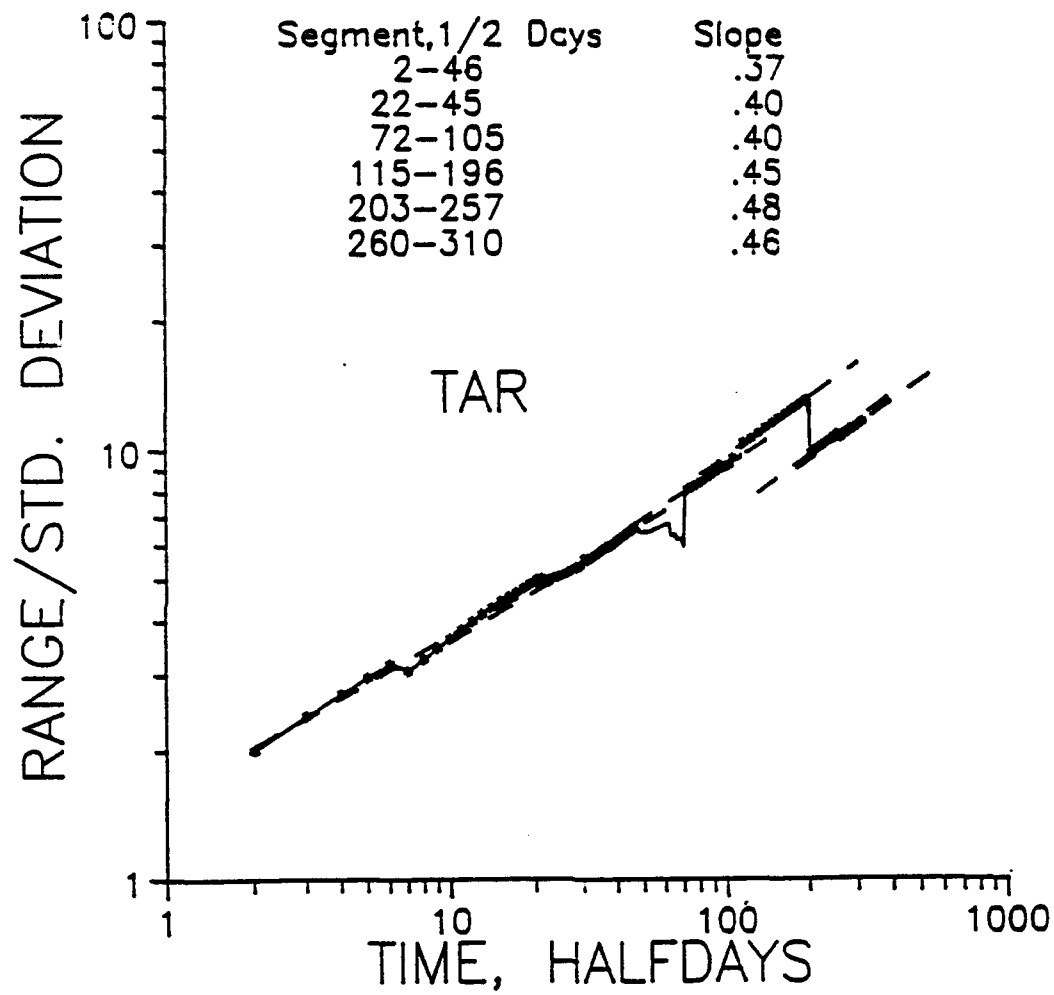


Figure 15

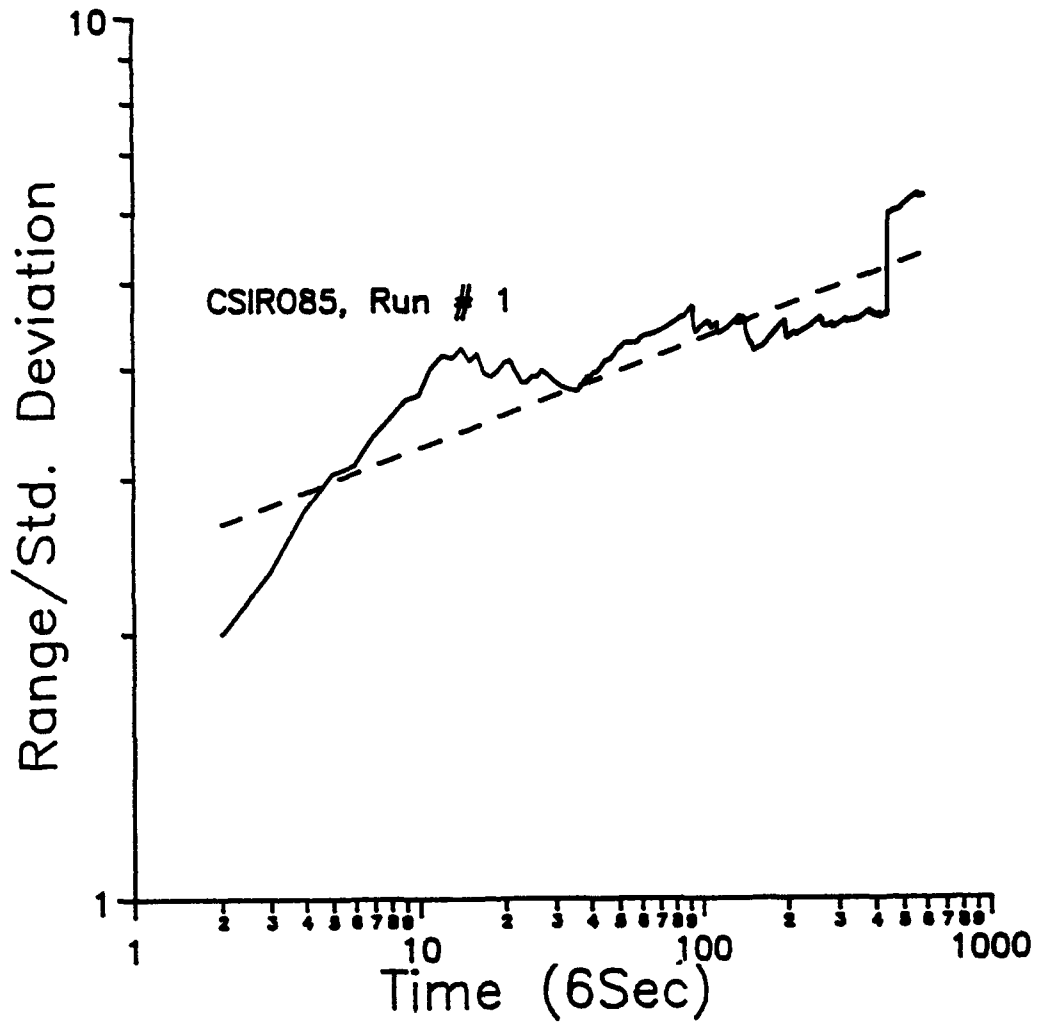


Figure 16

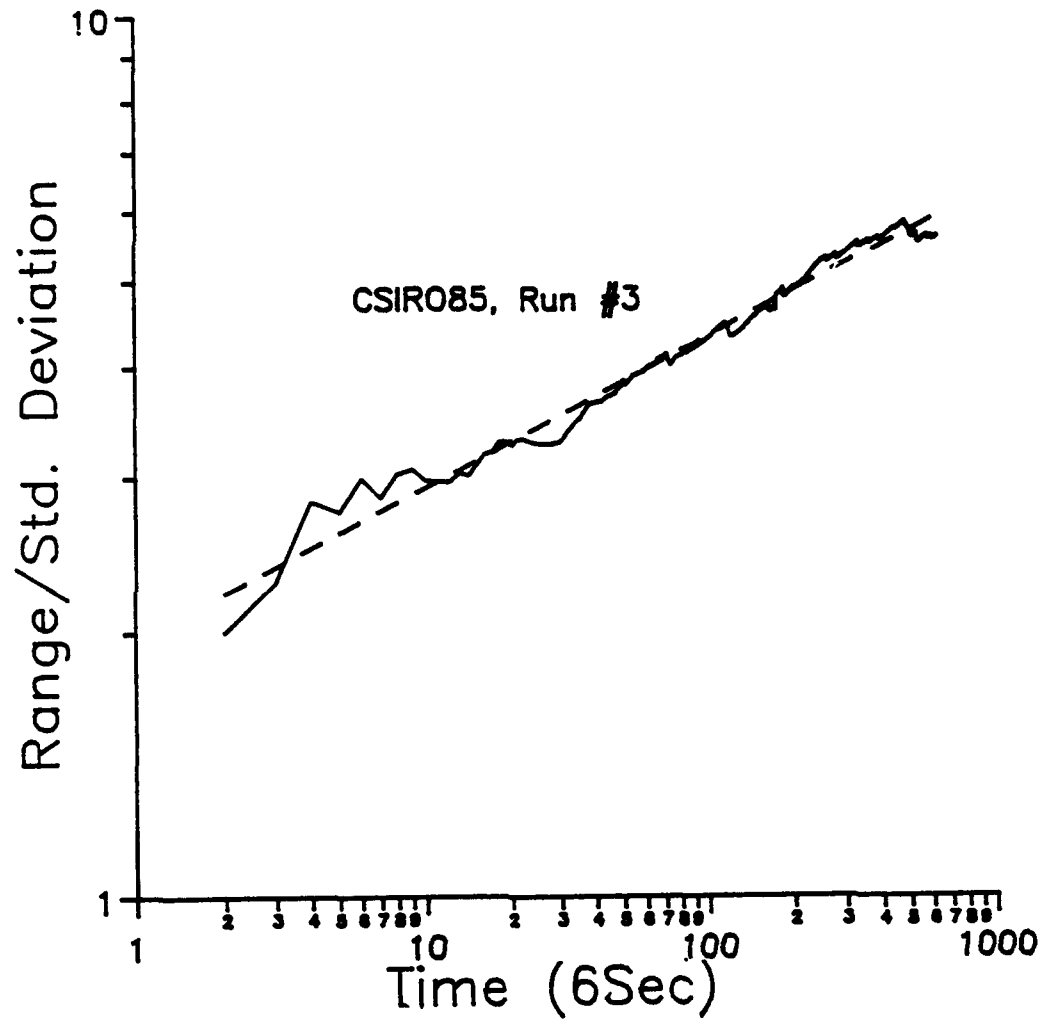


Figure 17

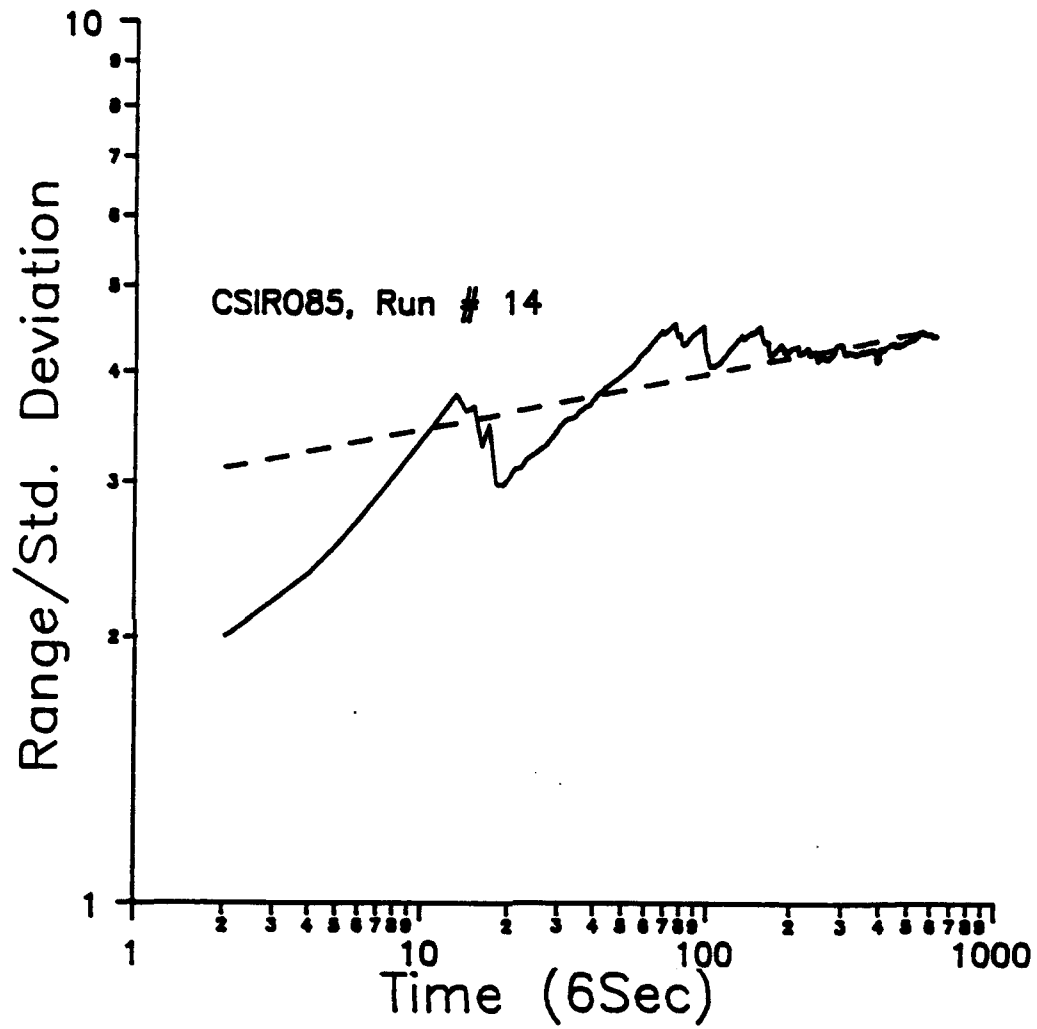


Figure 18

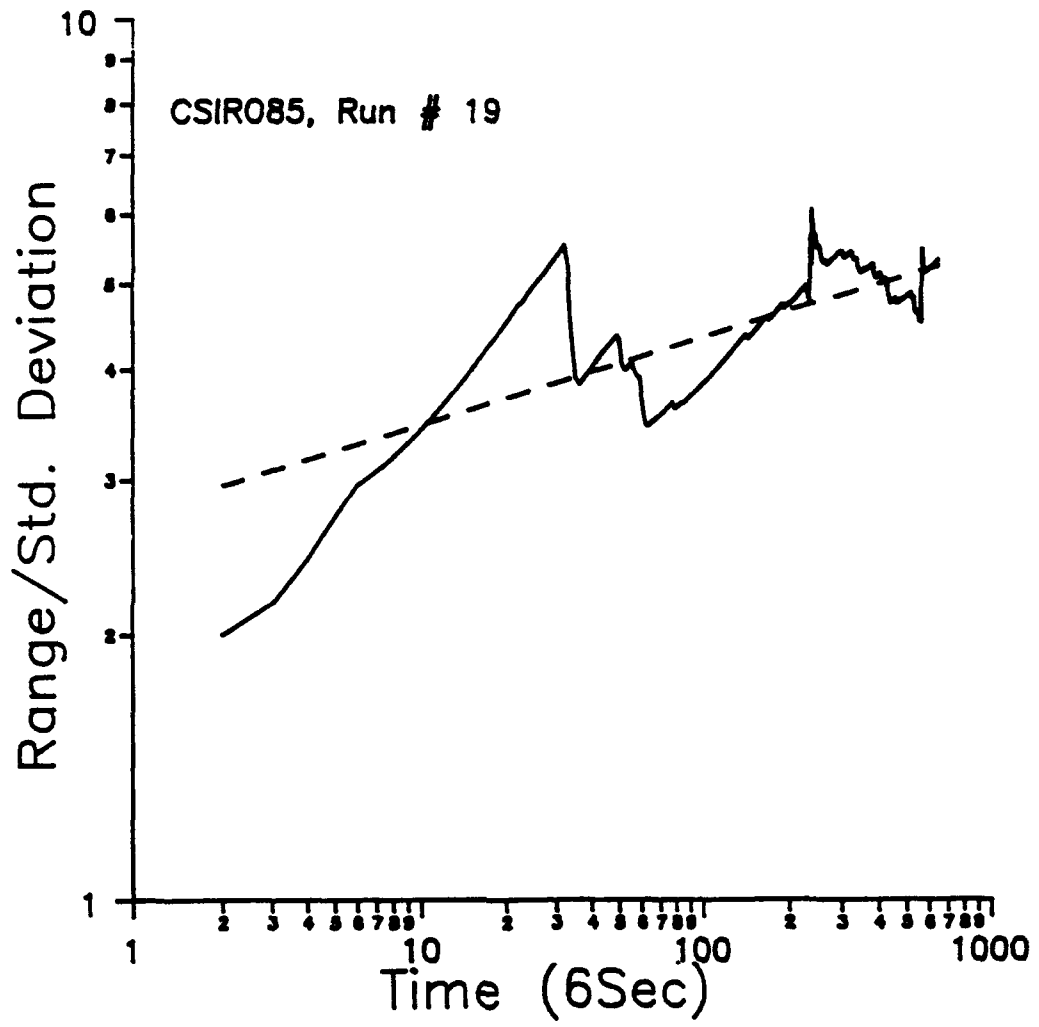


Figure 19

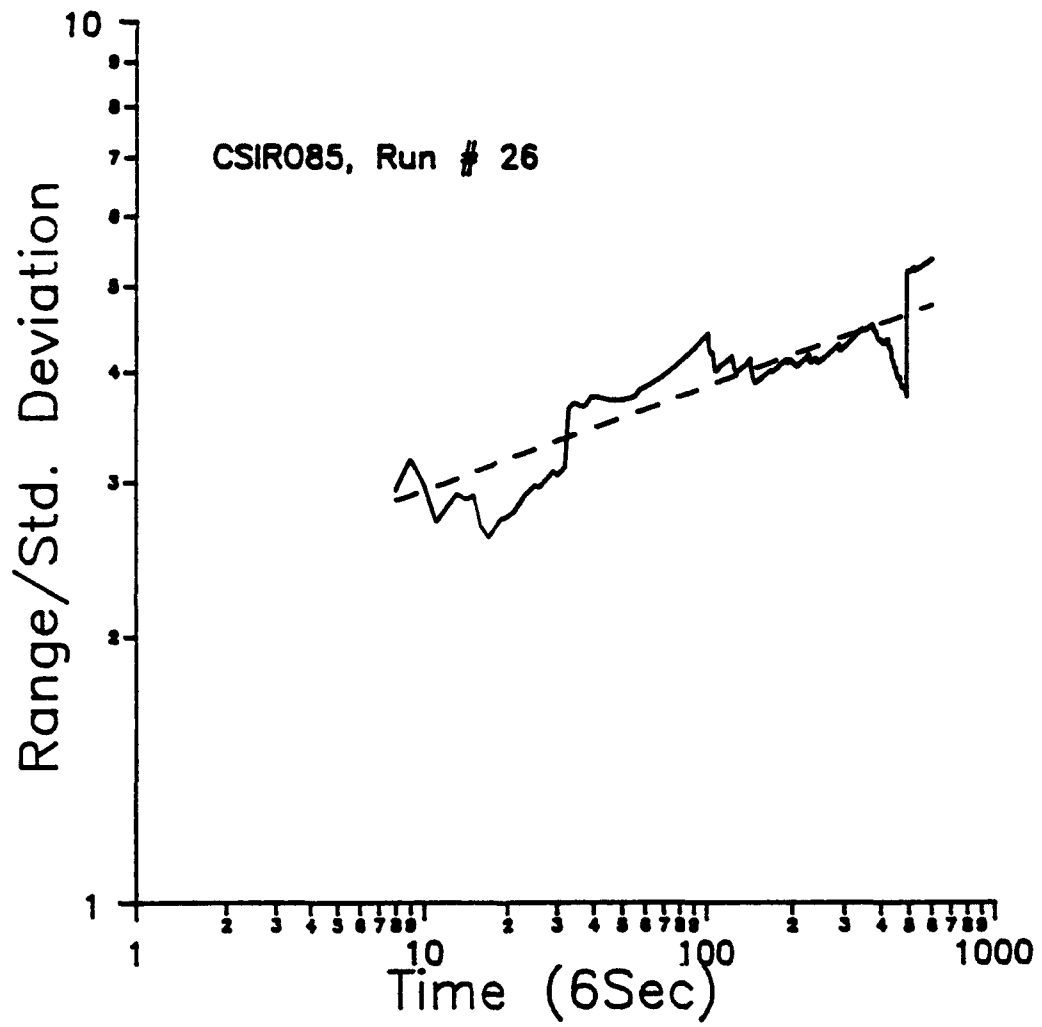


Figure 20

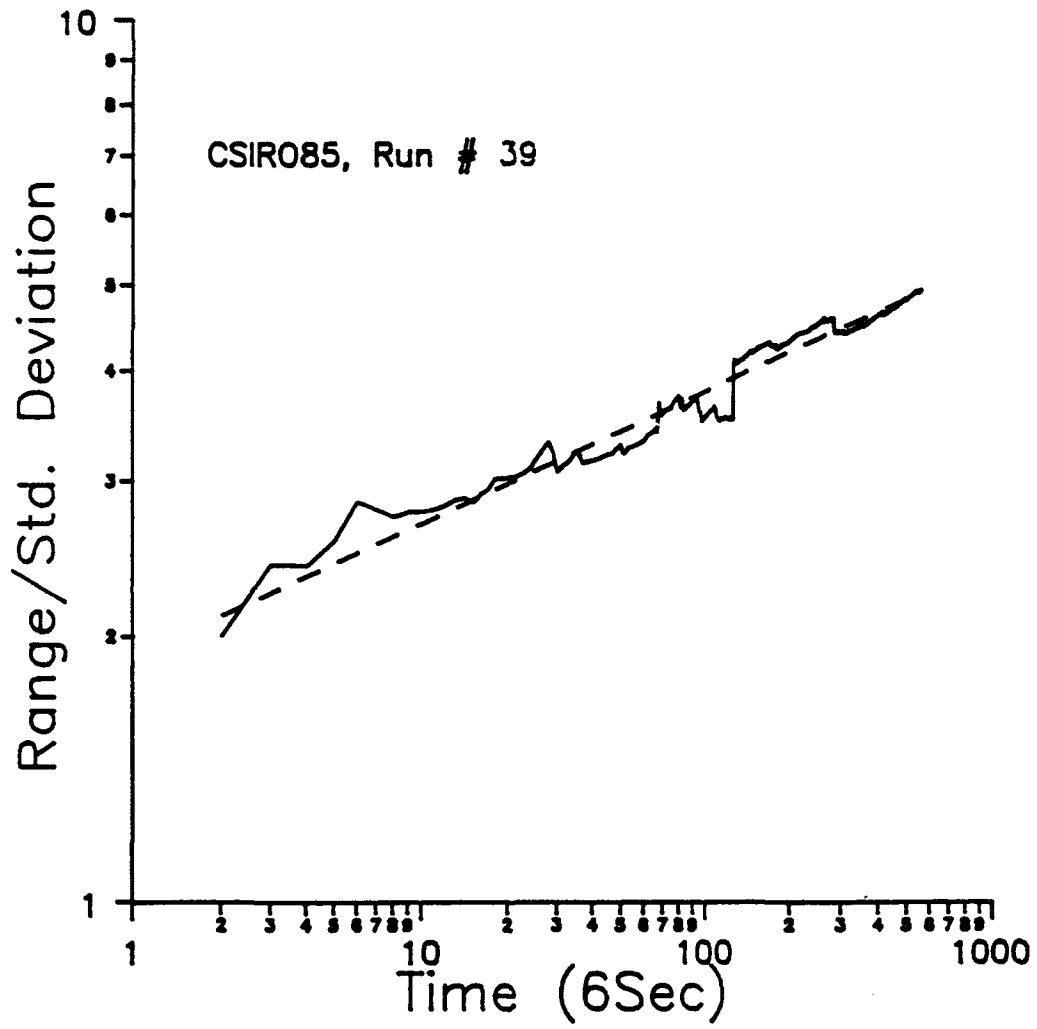


Figure 21

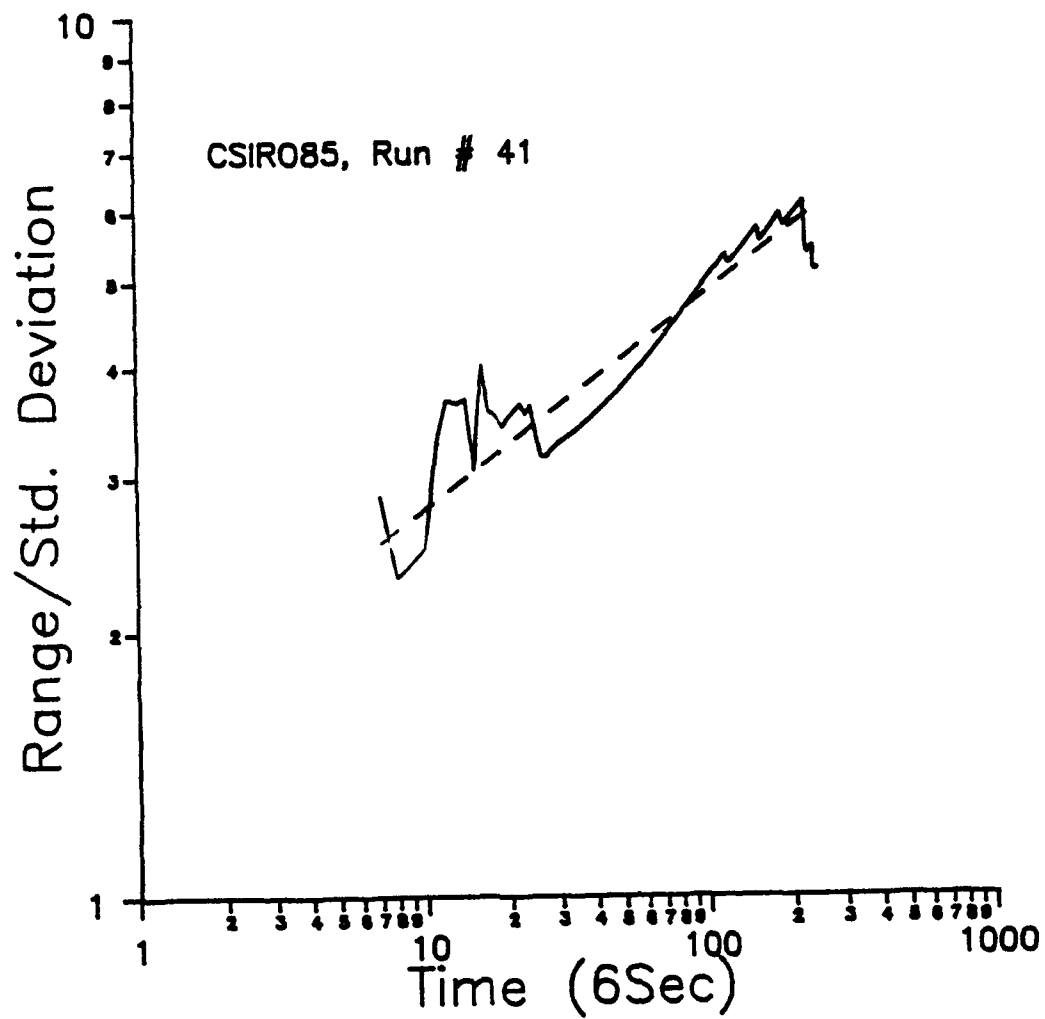


Figure 22

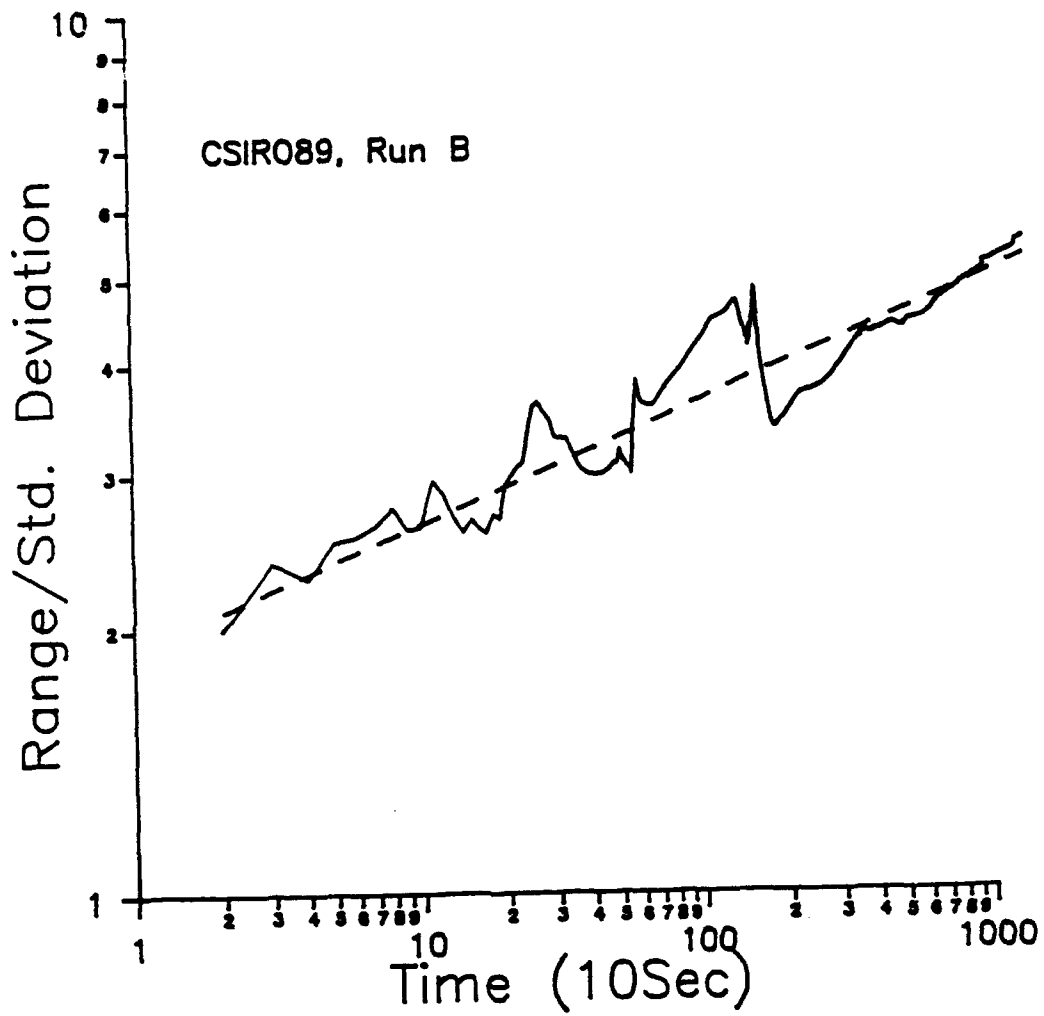


Figure 23

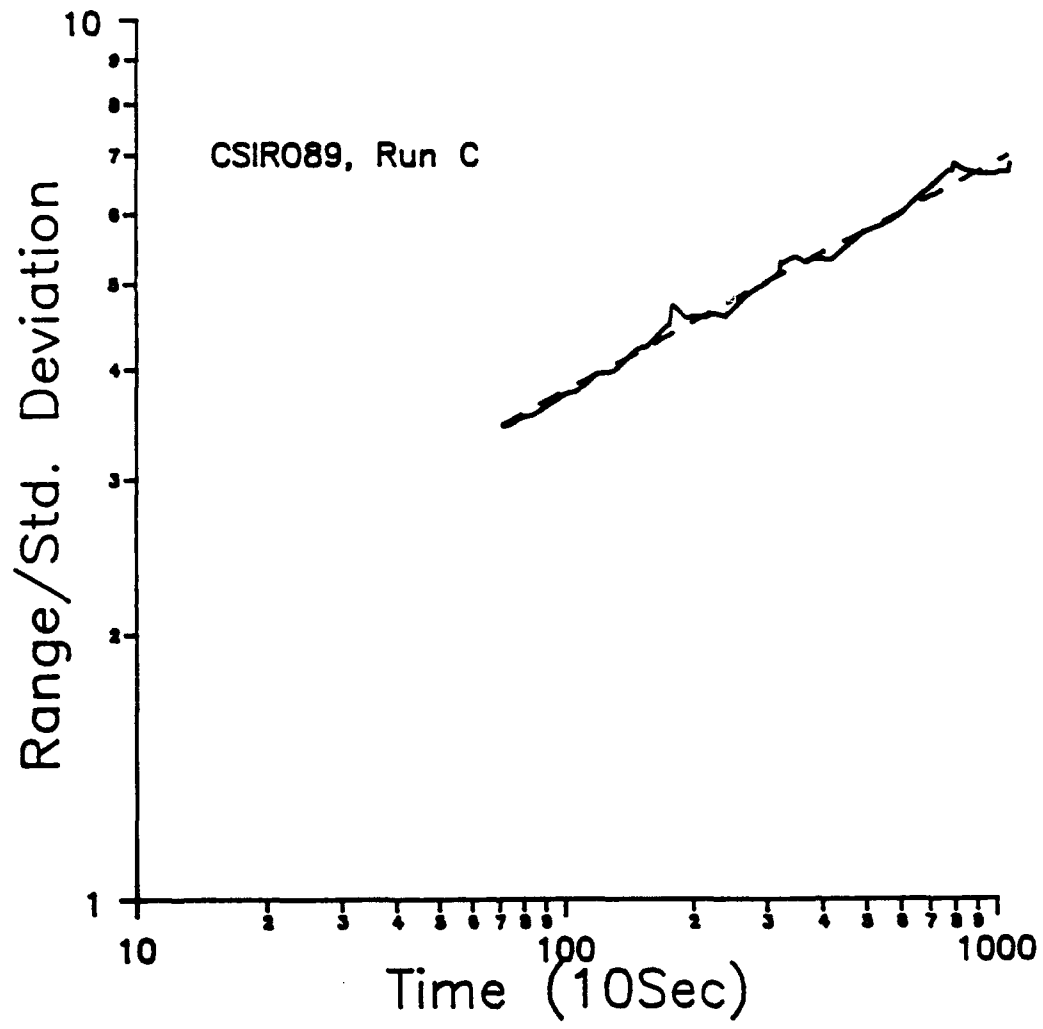


Figure 24

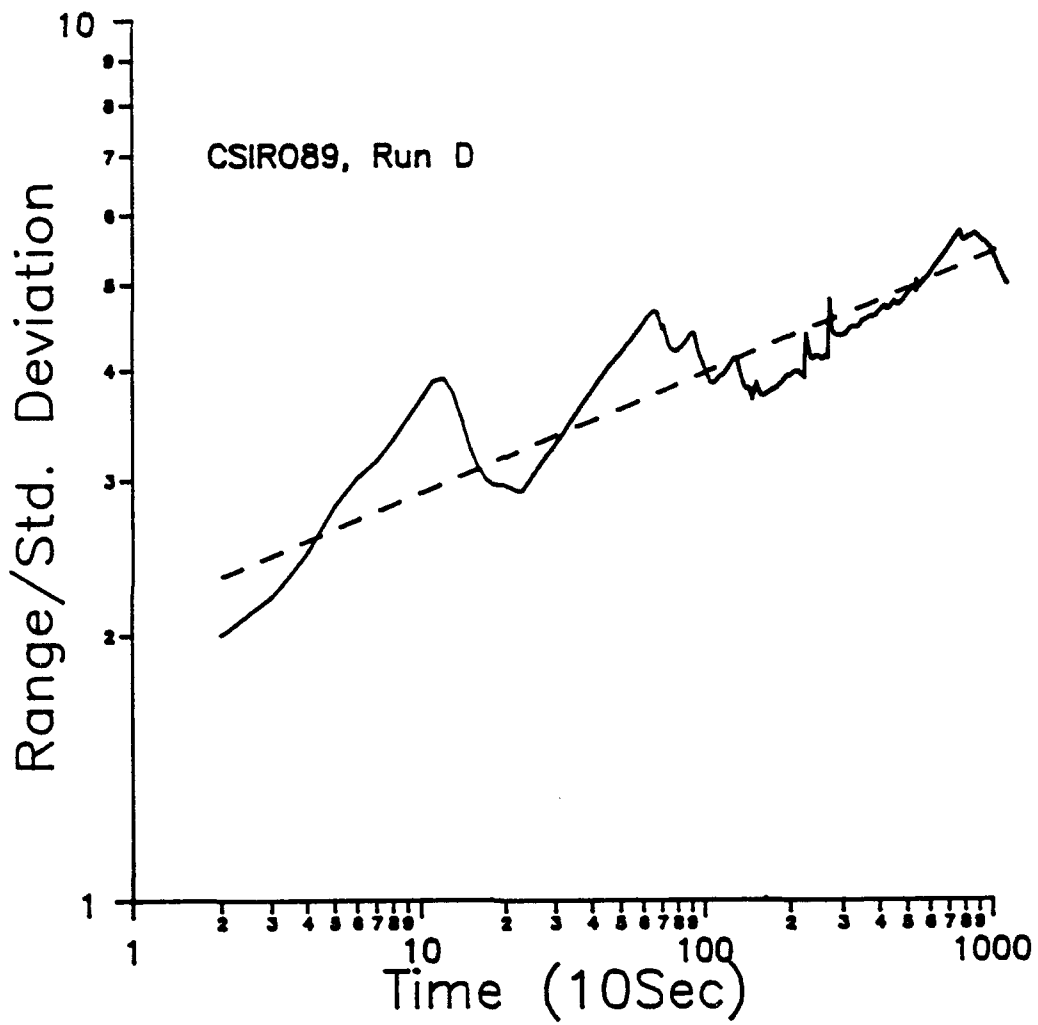


Figure 25

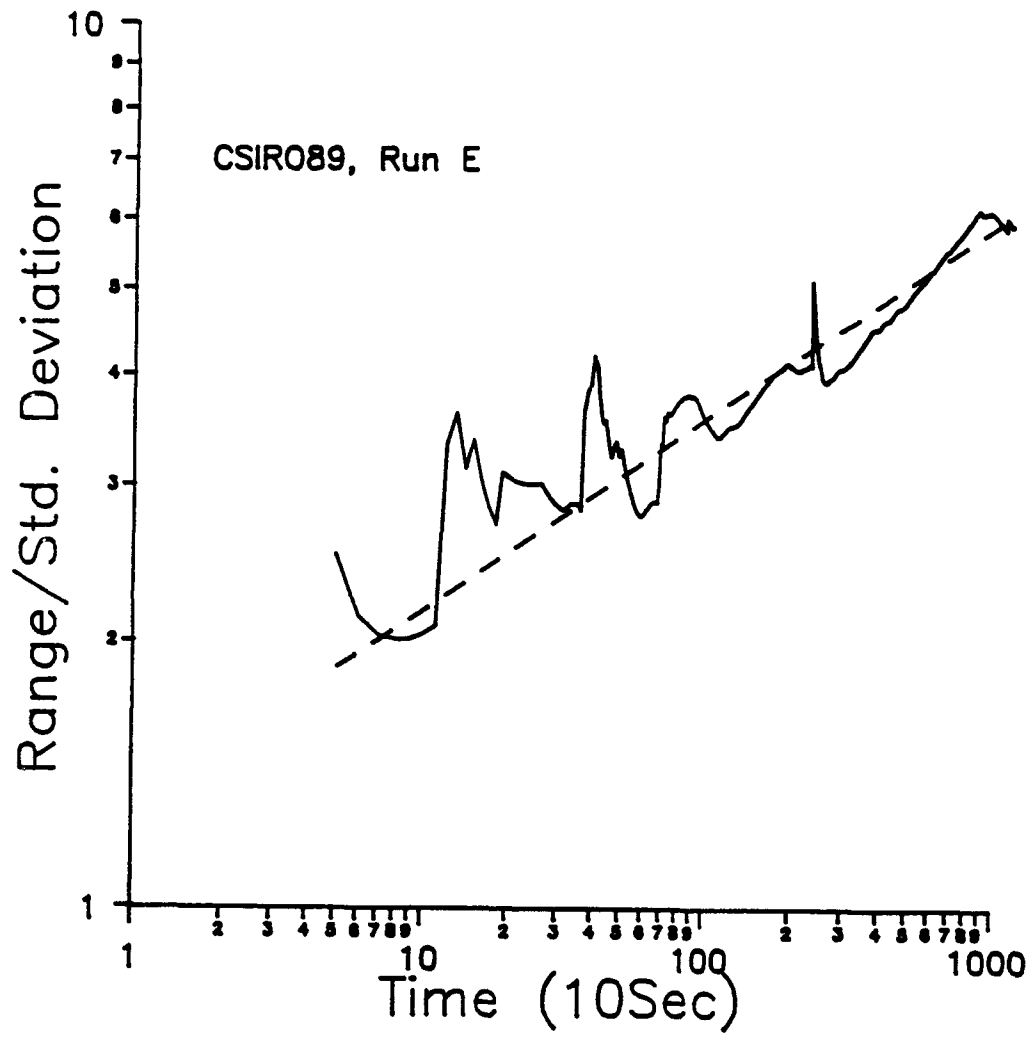


Figure 26

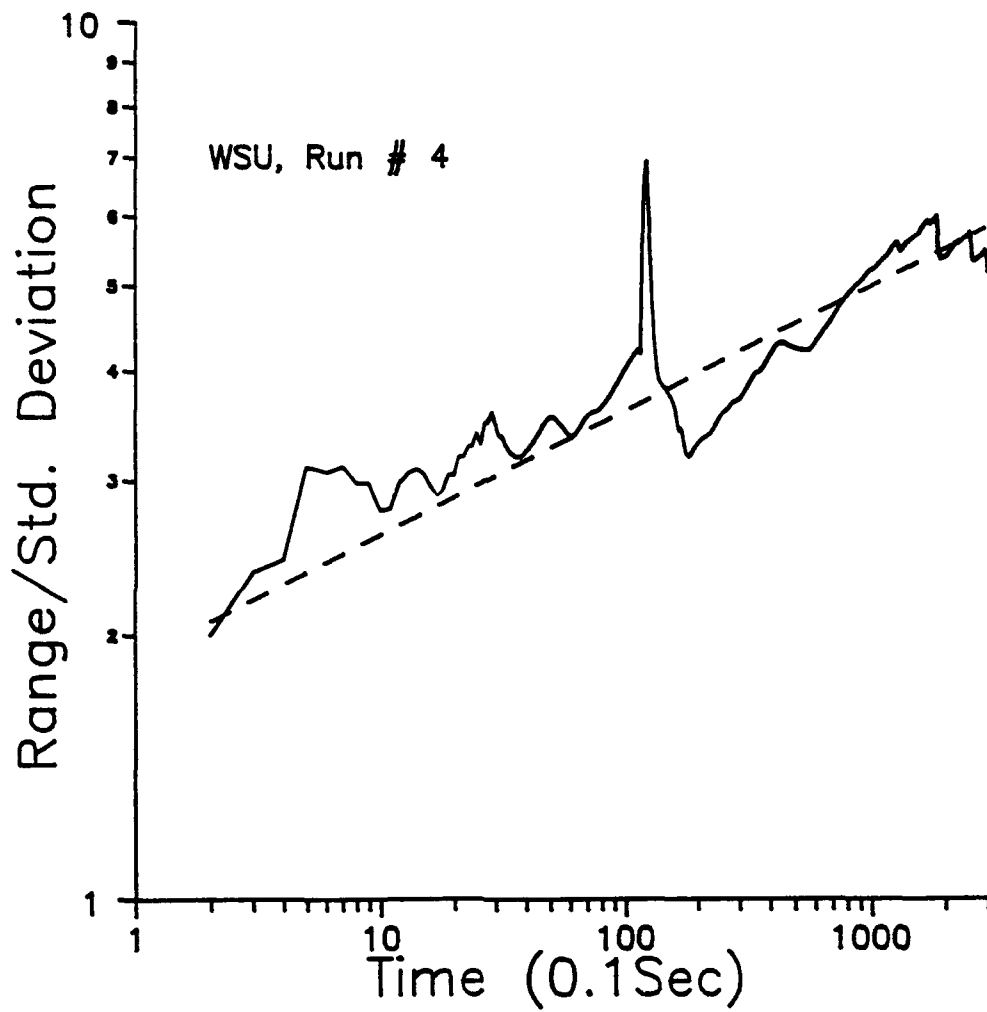


Figure 27

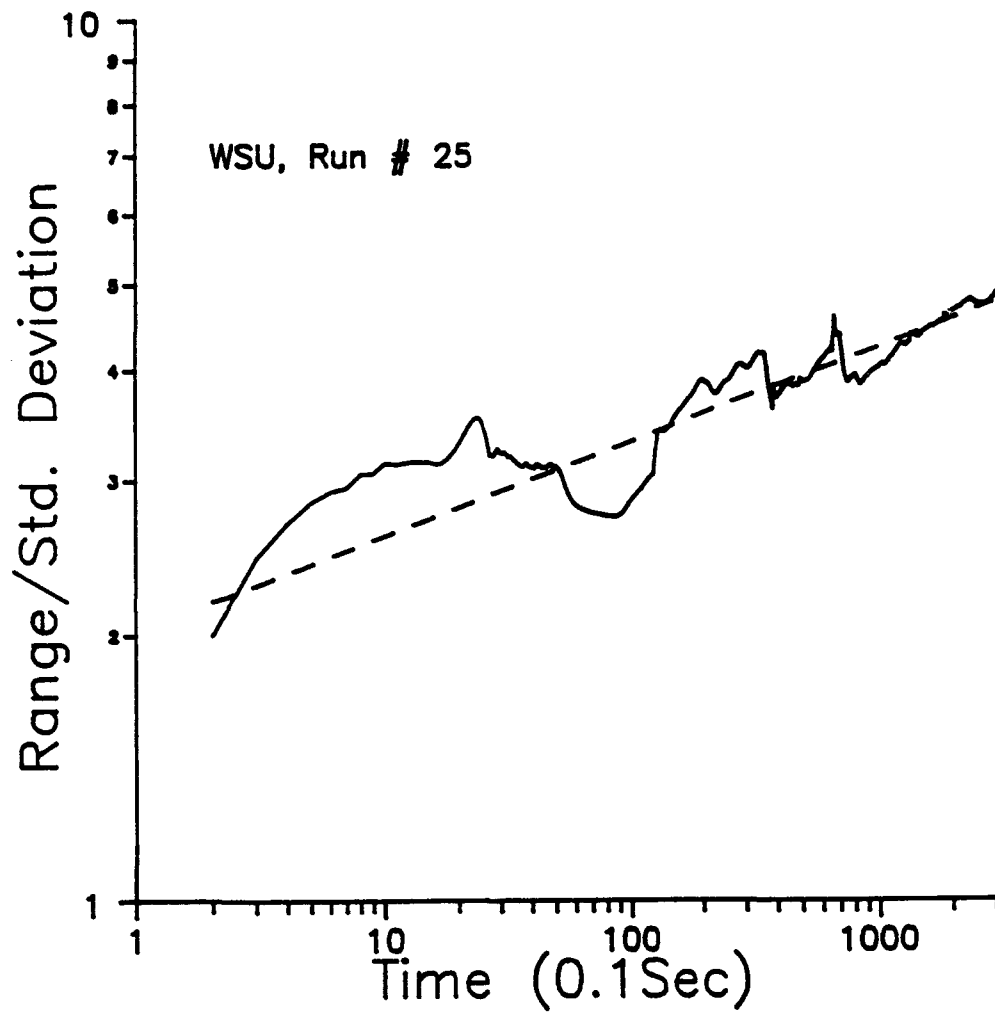


Figure 28

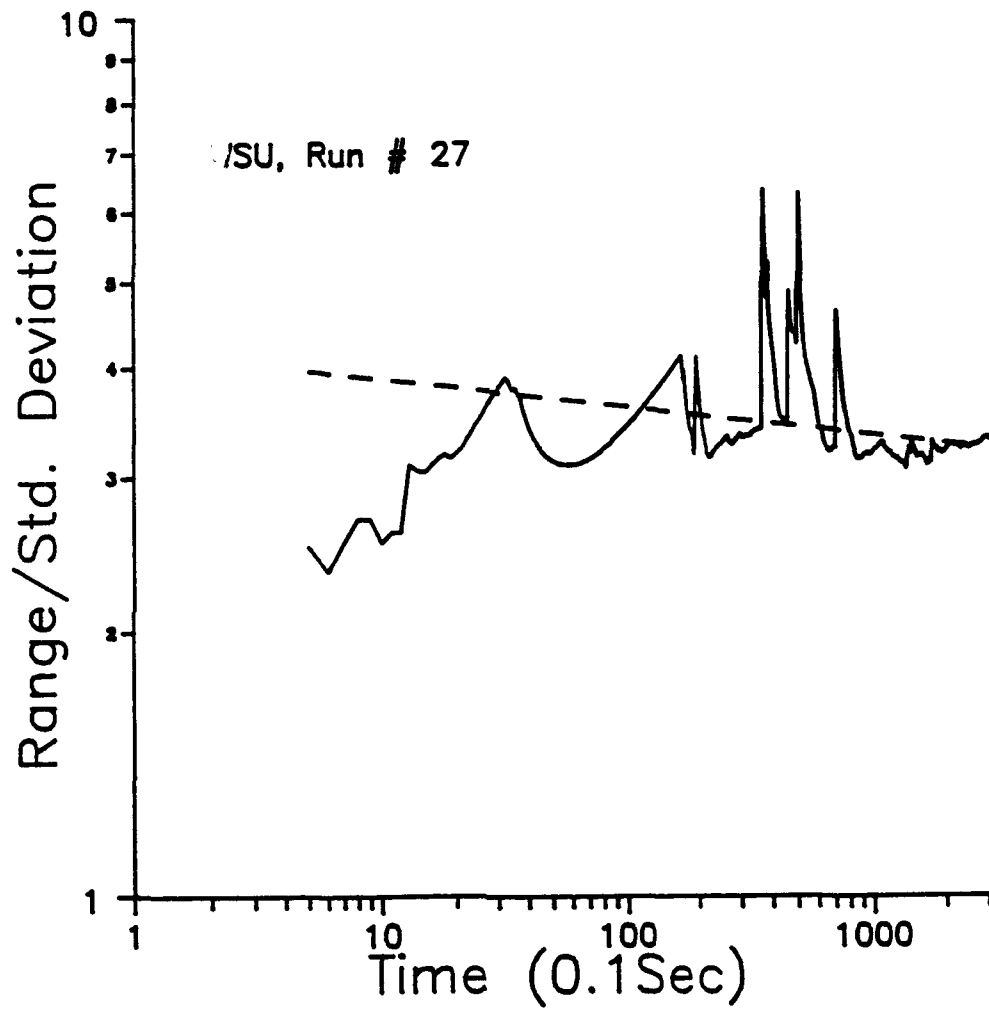


Figure 29

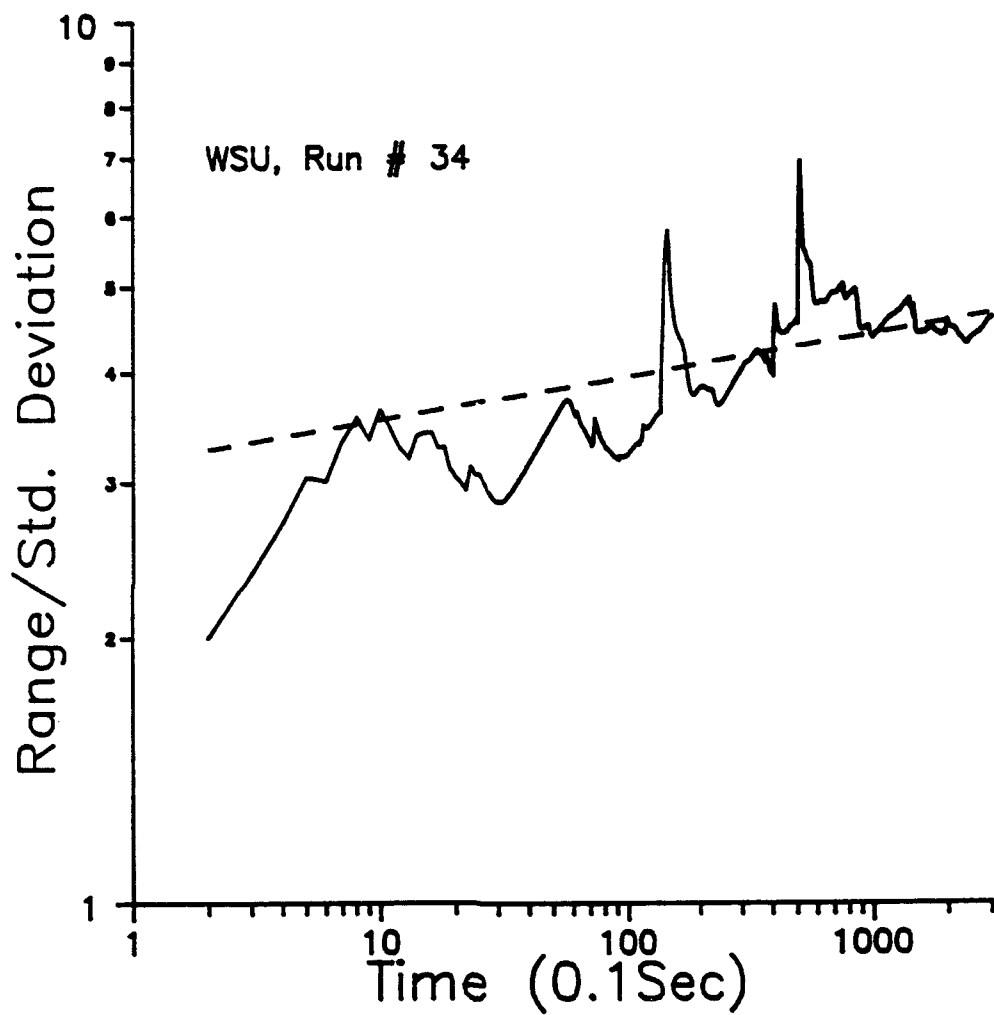


Figure 30

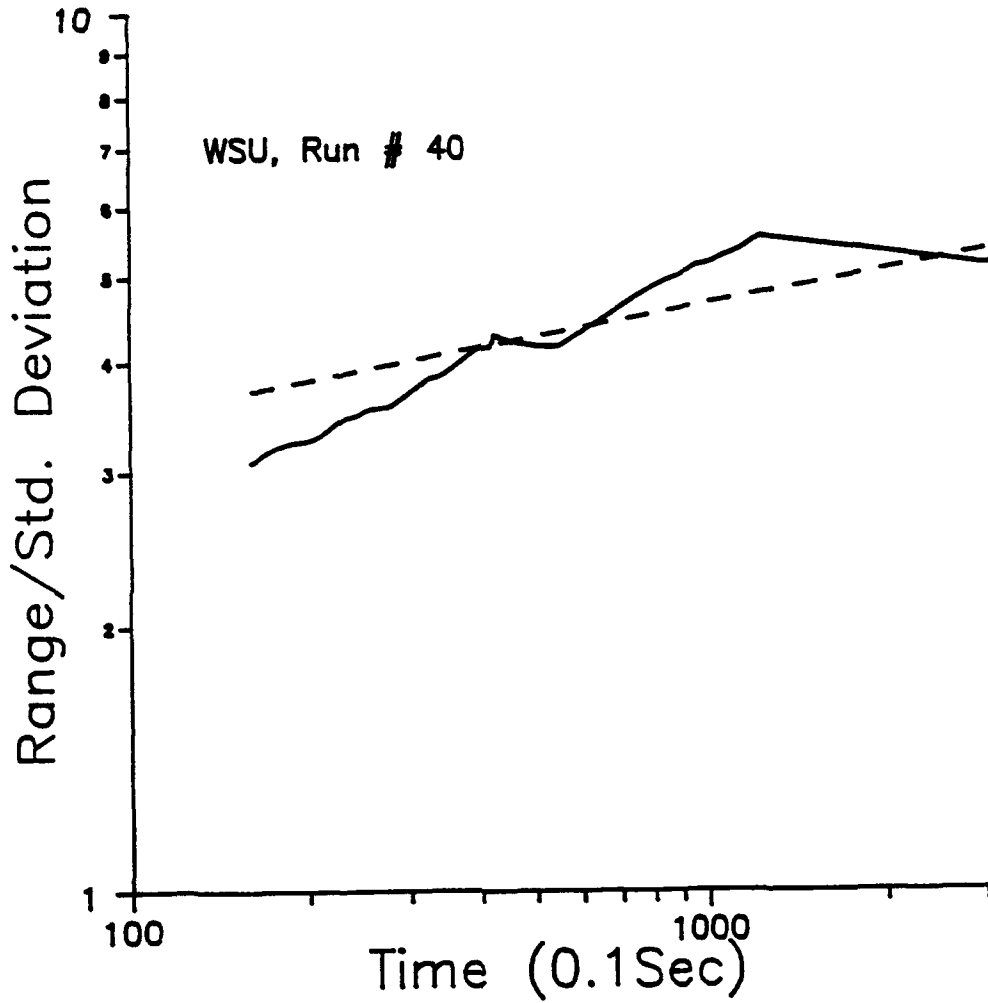


Figure 31

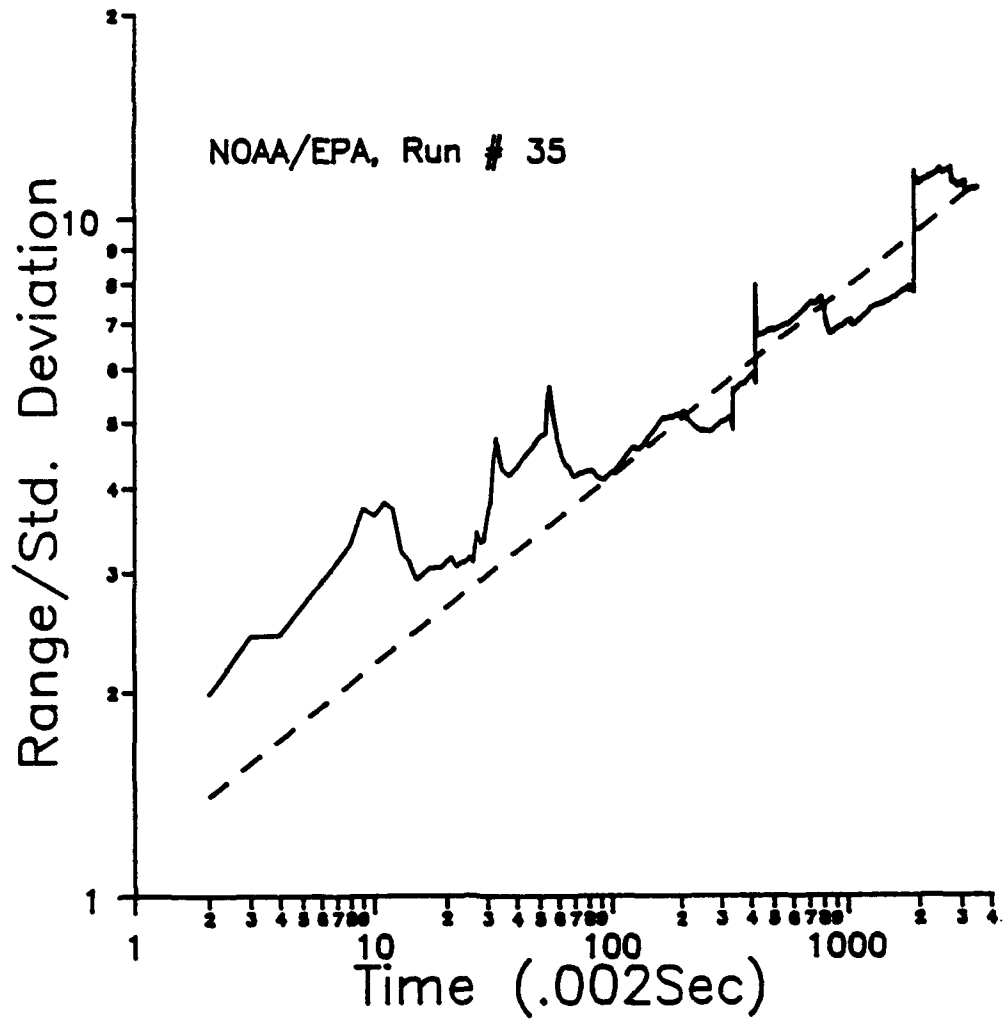


Figure 32

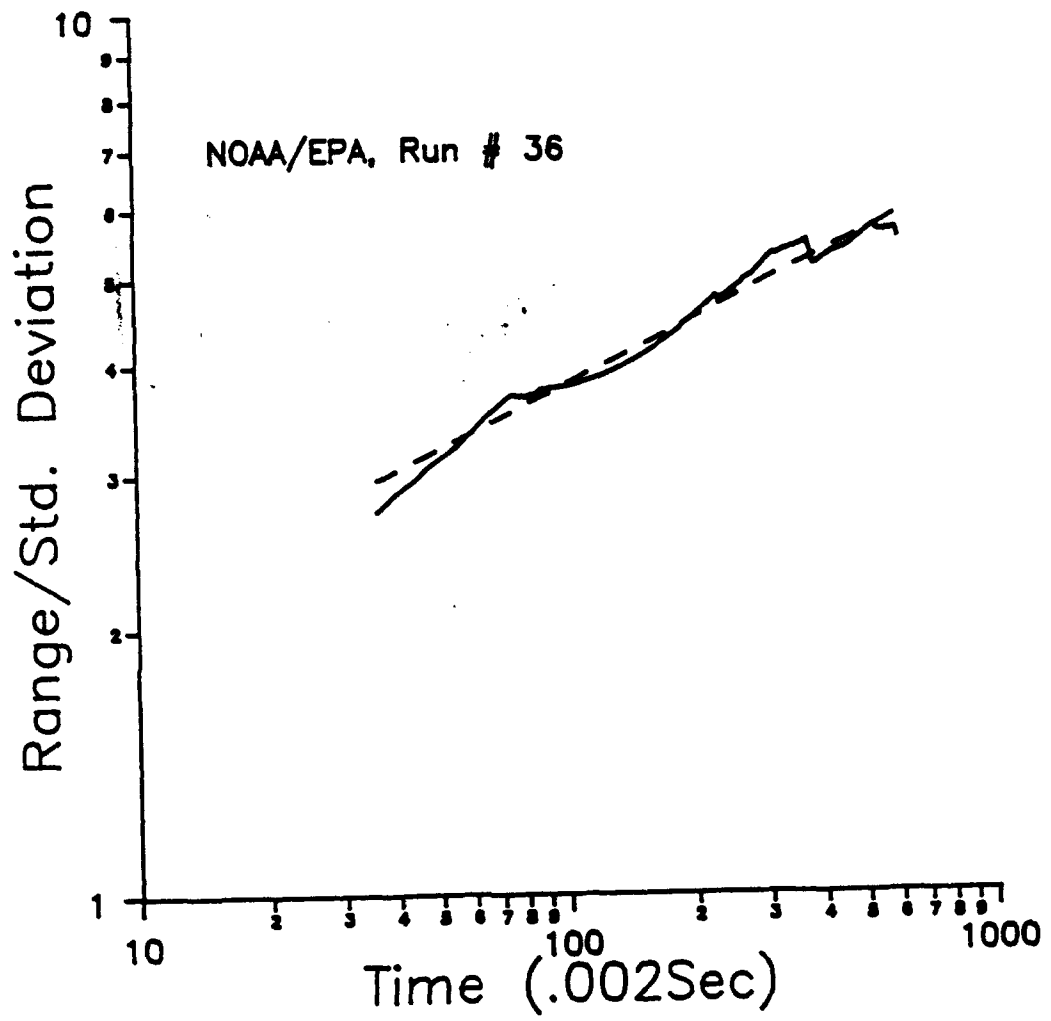


Figure 33